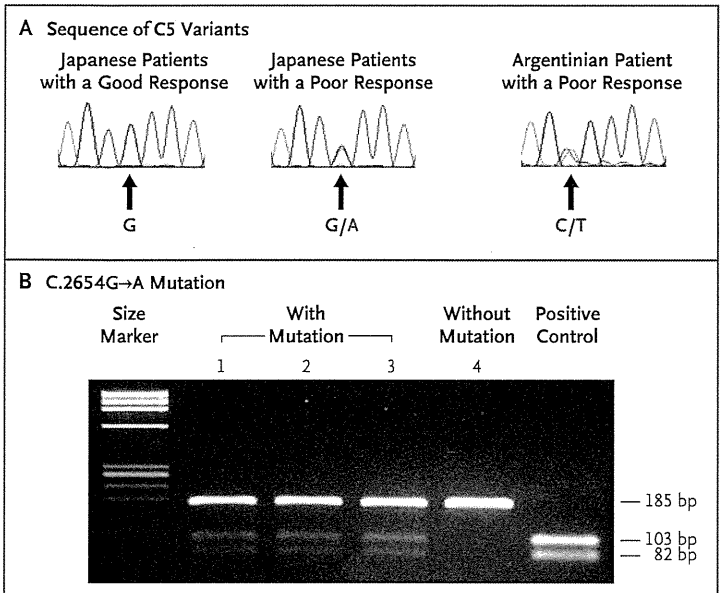

Figure 3. Genetic Variants of C5.

Panel A shows the sequence of the C5 variants detected in Japanese patients and an Argentinian patient with a poor response to eculizumab, as compared with the more frequently observed sequence in patients who had a good response to the drug. A heterozygous missense mutation in exon 21, c.2654G→A, predicting p.Arg885His, was identified in all Japanese patients with a poor response but not in those who had a good response. A very similar mutation, c.2653C→T, which predicts p.Arg885Cys, was identified in an Argentinian patient of Asian ancestry who had a poor response. Panel B shows a typical 2% agarose gel analysis to detect the presence of the c.2654G→A mutation. This mutation creates an *Apa*LI recognition site, which, when digested with *Apa*LI, generates the 185-bp polymerase-chain-reaction (PCR) product and two additional DNA fragments of 103 bp and 82 bp in length in heterozygous persons (lanes 1, 2, and 3). Lane 4 shows a PCR product from a homozygous sample without the mutation. The PCR product derived from a plasmid inserted with the mutant sequence was used as a positive control.

activity was completely suppressed in the patients with a good response (Fig. 1B).

These observations were corroborated through further study of the effect of exogenous eculizumab on the hemolytic activity in a serum sample obtained from a patient before administration of the drug. Although in vitro hemolytic activity in serum samples obtained from a healthy person and from a patient who had a good response to eculizumab was completely inhibited by eculizumab at serum concentrations of 6.25 μg per milliliter and 12.5 μg per milliliter, respectively, levels as high as 2000 μg of eculizumab per milliliter did not inhibit in vitro hemolysis in the serum samples obtained from the two patients who had a poor response (Fig. 2A). In contrast, results with N19-8, an antibody that binds a site on C5 that is distinct from the eculizumab binding site, showed that suppression of complement-mediated hemolysis was similar in the healthy person, the patient who had a good response to eculizumab, and the two patients who had a poor response (Fig. 2B).

C5 MUTATION IN JAPANESE PATIENTS WITH A POOR RESPONSE

We amplified all 41 exons of the C5 gene with primer sets specifically designed for each exon, using as a template genomic DNA prepared from mononuclear cells obtained from patients who had a poor response, and we directly sequenced all the PCR products from each exon (Fig. S1 in the Supplementary Appendix). We identified a single missense C5 heterozygous mutation at exon 21, c.2654G→A (DNA Data Bank of Japan accession number, AB860298), which predicts the polymorphism p.Arg885His, in both patients who had a poor response. This mutation was not seen in 7 patients who had a good response to eculizumab (Fig. 3A). In addition, we confirmed that 9 other Japanese patients who received treatment after completion of the AEGIS study and who had a poor response to eculizumab had the same C5 gene mutation (Table S1 in the Supplementary Appendix). The 11 patients with a poor response who had this mutation were identified among 345 Japanese patients who received eculizumab (rate of a poor response, 3.2%).

The c.2654G→A mutation generates a new *Apa*LI recognition site (Fig. S3 in the Supplementary Appendix); therefore, when digested with *Apa*LI, the 185-bp PCR product of exon 21 associated with nonmutant C5 generates two DNA fragments of 103 bp and 82 bp in length (Fig. 3B). However, the *Apa*LI digestion products from all 11 patients who had a poor response contained a mixture of the 185-, 103-, and 82-bp fragments; this confirms that each of these patients was heterozygous, with c.2654G→A in one allele and a nonmutant sequence in the other allele.

Next, we analyzed the prevalence of this mutation in the healthy Japanese population, using the gel-based assay in conjunction with DNA samples. We found that 10 of 288 healthy persons in Japan had the same heterozygous muta-

tion (3.5%), which is consistent with the prevalence we observed in the population of Japanese patients with PNH.

To determine the distribution of this polymorphism in other racial and ethnic populations, we screened several DNA panels. The c.2654G→A polymorphism was identified in 1 of 120 Han Chinese persons but was not seen in samples obtained from 100 persons of British ancestry and from 90 persons of Mexican ancestry.

MUTANT C5 IN JAPANESE PATIENTS WITH A POOR RESPONSE

To assess the influence of the genetic change on C5 function, electrophoretically pure rC5 and rC5m containing c.2654G→A were generated and functionally compared in various in vitro experiments. As a preliminary experiment, we confirmed that natural C5 (nC5), rC5, and rC5m restored classical-pathway lysis equivalently when added to C5-depleted serum (data not shown). Eculizumab did not block classical-pathway lysis in serum reconstituted with rC5m but did block rC5-dependent and nC5-dependent lysis (Fig. S4A in the Supplementary Appendix). By contrast, as observed with serum samples obtained from patients, N19-8 inhibited lysis in C5-depleted serum reconstituted with nC5, rC5, and rC5m (Fig. S4B in the Supplementary Appendix). Finally, although eculizumab bound nanomolar concentrations of rC5 on surface-plasmon-resonance analysis, with clear association and dissociation phases, there was no detectable binding with rC5m in the same assay up to the highest concentration of eculizumab (1 μM) examined (Fig. 4).

C5 MUTATION IN AN ARGENTINIAN PATIENT WITH A POOR RESPONSE

One patient with a poor response to eculizumab in whom the level of LDH remained markedly high during treatment with eculizumab was referred to us from Argentina. Although the known C5 polymorphism, c.2654G→A, was not identified in this patient, a new mutation, c.2653C→T, which predicts p.Arg885Cys, was detected in the base next to the known polymorphism (Fig. 3A).

To determine the prevalence and the distribution of this new variant, the same DNA panels described above were screened, but no mutation was identified in the 120 Han Chinese persons, the 100 persons of British ancestry, or the 90 persons of Mexican ancestry, suggesting that the prevalence of this variant might be too low to be detected in a sample of this size.

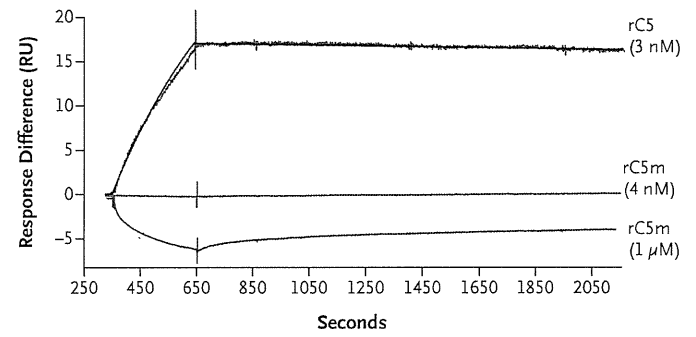

Figure 4. Effect of the Japanese C5 Polymorphism on the Functional Properties of C5.

Binding of eculizumab to recombinant C5 (rC5) with and without the mutation, as assessed by means of surface plasmon resonance, is shown. Eculizumab bound rC5 but did not bind mutant rC5 (rC5m) at concentrations below 5 nM. Increasing the concentration of eculizumab up to 1 μM did not elicit detectable binding to rC5m. A response unit (RU) is 1 pg of protein per square millimeter on a sensor surface. The vertical line at 650 seconds separates the on and off phases of the kinetics experiment (association of the analyte with dissociation from the ligand).

DISCUSSION

We identified a C5 mutation in Japanese patients with PNH. This mutation prevents binding and blockade by eculizumab while retaining the functional capacity of the mutant C5 to cause hemolysis.

Two patients with PNH enrolled in the AEGIS clinical trial did not have the characteristic response to eculizumab treatment, as shown by the lack of change in hemolytic markers such as levels of LDH. Serum samples obtained from these patients showed hemolytic activity even in the presence of high concentrations of exogenously added eculizumab. However, hemolytic activity was completely blocked by another anti-C5 monoclonal antibody (N19-8), which binds to a different site from that of eculizumab. A single missense C5 heterozygous mutation, c.2654G→A, was consistently detected in all 11 Japanese patients with a poor response and in none of the patients who had a good response. The prevalence of this polymorphism among patients with PNH (3.2%) was very similar to the prevalence

in healthy Japanese persons (3.5%), and the polymorphism has been identified in 1 of 120 Han Chinese persons. We then showed that the hemolytic activity supported by this structural variant in vitro was not blocked by eculizumab but was fully blocked by N19-8 and that the variant was incapable of binding eculizumab. Collectively, these data provide support for the hypothesis that the functional capacity of the mutant C5, together with its inability to bind to eculizumab, account for the poor response in patients who carry this mutation.

A new variant, c.2653C→T, which predicts p.Arg885Cys, was independently identified in an Argentinian patient of Asian ancestry, suggesting the importance of this site in C5 recognition by eculizumab and the racial and ethnic factors associated with this phenomenon. The Arg885His/Cys mutations are proximal to the C5 MG7 domain, close to the known epitope for binding of eculizumab[21] and within the contact region between the C5 convertase and bound C5 substrate, as inferred by Laursen et al.[22] Evidently, these mutations, in keeping with the high specificity of monoclonal antibody binding, disrupt the eculizumab epitope but maintain the capacity of C5m to undergo cleavage by the C5 convertase. Therefore, we conclude that the poor response to eculizumab in a subgroup of Japanese patients is explained by the inability of a subset of lysis-competent C5 in these patients to bind and undergo blockade by the drug. The polymorphism in the target protein might be important to consider in patients with a poor response to other antibody-based treatments for various diseases.[23-25]

Supported by Alexion Pharmaceuticals and a grant from the Research Committee for the Idiopathic Hematopoietic Disorders, Ministry of Health, Labor, and Welfare of Japan (H23-Nanchi-Japan-001).

Disclosure forms provided by the authors are available with the full text of this article at NEJM.org.

We thank the following employees of Alexion Pharmaceuticals for technical support: Richard Altman and Doug Sheridan (for assistance with protein expression), Fang Sun (for assistance with protein purification), Rekha Patel (for assistance with surface-plasmon-resonance analysis), and Gerard Graminski (for assistance with bioanalytical assays); Drs. Yoshiko Murakami and Yusuke Maeda, both of Osaka University, Japan, for advice and critical discussions; and Dr. Otto Götze of the Department of Immunology, University of Göttingen, Germany, for supplying the hybridoma cells for N19-8.

REFERENCES

1. Miyata T, Takeda J, Iida Y, et al. The cloning of PIG-A, a component in the early step of GPI-anchor biosynthesis. Science 1993;259:1318-20.
2. Takeda J, Miyata T, Kawagoe K, et al. Deficiency of the GPI anchor caused by a somatic mutation of the PIG-A gene in paroxysmal nocturnal hemoglobinuria. Cell 1993;73:703-11.
3. Miyata T, Yamada N, Iida Y, et al. Abnormalities of PIG-A transcripts in granulocytes from patients with paroxysmal nocturnal hemoglobinuria. N Engl J Med 1994;330:249-55.
4. Parker C, Omine M, Richards S, et al. Diagnosis and management of paroxysmal nocturnal hemoglobinuria. Blood 2005;106:3699-709.
5. Brodsky RA. How I treat paroxysmal nocturnal hemoglobinuria. Blood 2009; 113:6522-7.
6. Luzzatto L, Gianfaldoni G, Notaro R. Management of paroxysmal nocturnal haemoglobinuria: a personal view. Br J Haematol 2011;153:709-20.
7. Hillmen P, Lewis SM, Bessler M, Luzzatto L, Dacie JV. Natural history of paroxysmal nocturnal hemoglobinuria. N Engl J Med 1995;333:1253-8.
8. Socié G, Mary JY, de Gramont A, et al. Paroxysmal nocturnal haemoglobinuria: long-term follow-up and prognostic factors. Lancet 1996;348:573-7.
9. Nishimura J, Kanakura Y, Ware RE, et al. Clinical course and flow cytometric analysis of paroxysmal nocturnal hemoglobinuria in the United States and Japan. Medicine (Baltimore) 2004;83:193-207.
10. Rother RP, Rollins SA, Mojcik CF, Brodsky RA, Bell L. Discovery and development of the complement inhibitor eculizumab for the treatment of paroxysmal nocturnal hemoglobinuria. Nat Biotechnol 2007;25:1256-64. [Erratum, Nat Biotechnol 2007;25:1488.]
11. Parker C. Eculizumab for paroxysmal nocturnal haemoglobinuria. Lancet 2009; 373:759-67.
12. Hillmen P, Hall C, Marsh JC, et al. Effect of eculizumab on hemolysis and transfusion requirements in patients with paroxysmal nocturnal hemoglobinuria. N Engl J Med 2004;350:552-9.
13. Hill A, Hillmen P, Richards SJ, et al. Sustained response and long-term safety of eculizumab in paroxysmal nocturnal hemoglobinuria. Blood 2005;106:2559-65.
14. Hillmen P, Young NS, Schubert J, et al. The complement inhibitor eculizumab in paroxysmal nocturnal hemoglobinuria. N Engl J Med 2006;355:1233-43.
15. Hillmen P, Muus P, Dührsen U, et al. Effect of the complement inhibitor eculizumab on thromboembolism in patients with paroxysmal nocturnal hemoglobinuria. Blood 2007;110:4123-8.
16. Brodsky RA, Young NS, Antonioli E, et al. Multicenter phase 3 study of the complement inhibitor eculizumab for the treatment of patients with paroxysmal nocturnal hemoglobinuria. Blood 2008; 111:1840-7.
17. Kanakura Y, Ohyashiki K, Shichishima T, et al. Safety and efficacy of the terminal complement inhibitor eculizumab in Japanese patients with paroxysmal nocturnal hemoglobinuria: the AEGIS clinical trial. Int J Hematol 2011;93:36-46.
18. Risitano AM, Notaro R, Marando L, et al. Complement fraction 3 binding on erythrocytes as additional mechanism of disease in paroxysmal nocturnal hemoglobinuria patients treated by eculizumab. Blood 2009;113:4094-100.
19. Würzner R, Schulze M, Happe L, et al. Inhibition of terminal complement complex formation and cell lysis by monoclonal antibodies. Complement Inflamm 1991;8:328-40.
20. van den Berg CW. Purification of complement components, regulators, and receptors by classical methods. Methods Mol Biol 2000;150:15-52.
21. Zuber J, Fakhouri F, Roumenina LT, Loirat C, Frémeaux-Bacchi V. Use of eculizumab for atypical haemolytic uraemic syndrome and C3 glomerulopathies. Nat Rev Nephrol 2012;8:643-57.
22. Laursen NS, Andersen KR, Braren I,

Spillner E, Sottrup-Jensen L, Andersen GR. Substrate recognition by complement convertases revealed in the C5-cobra venom factor complex. EMBO J 2011;30:606-16.
23. Wu J, Edberg JC, Redecha PB, et al. A novel polymorphism of FcgammaRIIIa (CD16) alters receptor function and predisposes to autoimmune disease. J Clin Invest 1997;100:1059-70.
24. Cartron G, Dacheux L, Salles G, et al. Therapeutic activity of humanized anti-CD20 monoclonal antibody and polymorphism in IgG Fc receptor FcgammaRIIIa gene. Blood 2002;99:754-8.
25. Treon SP, Hansen M, Branagan AR, et al. Polymorphisms in FcgammaRIIIA (CD16) receptor expression are associated with clinical response to rituximab in Waldenström's macroglobulinemia. J Clin Oncol 2005;23:474-81.

JVI Journals.ASM.org

Generation of Rhesus Macaque-Tropic HIV-1 Clones That Are Resistant to Major Anti-HIV-1 Restriction Factors

Masako Nomaguchi,[a] Masaru Yokoyama,[b] Ken Kono,[c] Emi E. Nakayama,[c] Tatsuo Shioda,[c] Naoya Doi,[a,d] Sachi Fujiwara,[a] Akatsuki Saito,[d,e] Hirofumi Akari,[e] Kei Miyakawa,[d,f] Akihide Ryo,[f] Hirotaka Ode,[d,g] Yasumasa Iwatani,[g] Tomoyuki Miura,[h] Tatsuhiko Igarashi,[h] Hironori Sato,[b] Akio Adachi[a]

Department of Microbiology, Institute of Health Biosciences, The University of Tokushima Graduate School, Tokushima, Tokushima, Japan[a]; Laboratory of Viral Genomics, Pathogen Genomics Center, National Institute of Infectious Diseases, Musashimurayama, Tokyo, Japan[b]; Department of Viral Infections, Research Institute for Microbial Diseases, Osaka University, Suita, Osaka, Japan[c]; Japanese Foundation for AIDS Prevention, Chiyoda-ku, Tokyo, Japan[d]; Section of Comparative Immunology and Microbiology, Center for Human Evolution Modeling Research, Primate Research Institute, Kyoto University, Inuyama, Aichi, Japan[e]; Department of Microbiology, Yokohama City University School of Medicine, Yokohama, Kanagawa, Japan[f]; Clinical Research Center, Department of Infectious Diseases and Immunology, National Hospital Organization Nagoya Medical Center, Nagoya, Aichi, Japan[g]; Laboratory of Primate Model, Experimental Research Center for Infectious Diseases, Institute for Virus Research, Kyoto University, Kyoto, Kyoto, Japan[h]

Human immunodeficiency virus type 1 (HIV-1) replication in macaque cells is restricted mainly by antiviral cellular APOBEC3, TRIM5α/TRIM5CypA, and tetherin proteins. For basic and clinical HIV-1/AIDS studies, efforts to construct macaque-tropic HIV-1 (HIV-1mt) have been made by us and others. Although rhesus macaques are commonly and successfully used as infection models, no HIV-1 derivatives suitable for *in vivo* rhesus research are available to date. In this study, to obtain novel HIV-1mt clones that are resistant to major restriction factors, we altered Gag and Vpu of our best HIV-1mt clone described previously. First, by sequence- and structure-guided mutagenesis, three amino acid residues in Gag-capsid (CA) (M94L/R98S/G114Q) were found to be responsible for viral growth enhancement in a macaque cell line. Results of *in vitro* TRIM5α susceptibility testing of HIV-1mt carrying these substitutions correlated well with the increased viral replication potential in macaque peripheral blood mononuclear cells (PBMCs) with different *TRIM5* alleles, suggesting that the three amino acids in HIV-1mt CA are involved in the interaction with TRIM5α. Second, we replaced the transmembrane domain of Vpu of this clone with the corresponding region of simian immunodeficiency virus SIVgsn166 Vpu. The resultant clone, MN4/LSDQgtu, was able to antagonize macaque but not human tetherin, and its Vpu effectively functioned during viral replication in a macaque cell line. Notably, MN4/LSDQgtu grew comparably to SIVmac239 and much better than any of our other HIV-1mt clones in rhesus macaque PBMCs. In sum, MN4/LSDQgtu is the first HIV-1 derivative that exhibits resistance to the major restriction factors in rhesus macaque cells.

Human immunodeficiency virus type 1 (HIV-1) has spread globally in human populations following cross-species transmission of simian immunodeficiency virus (SIV) from chimpanzees (1, 2). HIV-1 replicates well in humans and causes disease-inducing persistent infection only in humans. HIV-1 infection is impeded after virus entry in rhesus macaques (RhMs) and cynomolgus macaques (CyMs), which are frequently used for experimental viral infection studies (3). The block of HIV-1 infection in macaque cells is attributable to intrinsic restriction factors, including APOBEC3, TRIM5α/TRIM5CypA, and tetherin proteins (1, 4–6). These factors exert their antiretroviral activity in a species-specific manner, and HIV-1 effectively subverts their counterparts in human cells (1, 4–6). In contrast, a standard pathogenic clone, SIVmac239, for AIDS model studies evades the restriction factors and replicates well in macaques. HIV-1 and SIVmac239 are mutually related primate lentiviruses and cause AIDS in their respective hosts. Nevertheless, there are significant differences between the two viruses in genome organization, the viral replication profile *in vivo*, and disease progression (7–9). It is therefore most preferable to generate pathogenic HIV-1 derivatives to establish AIDS macaque models (7–9). Importantly, construction of HIV-1 derivatives that overcome the species barrier would contribute much to the understanding of the molecular interaction of viral and host proteins.

Of the intrinsic restriction factors in macaque cells, major determinants of the HIV-1 host range are the APOBEC3 and TRIM5 proteins (4, 8, 10). APOBEC3G is the strongest inhibitor of HIV-1 replication among APOBEC3 family proteins. It exhibits cytidine deaminase activity and causes hypermutation in the HIV-1 genome following incorporation into progeny virions in producer cells. HIV-1 Vif is able to degrade human APOBEC3G and neutralize its antiviral activity but is not effective against macaque APOBEC3G (4–6, 11, 12). Macaque TRIM5 proteins recognize and interact with the incoming HIV-1 cores and inhibit viral infection prior to reverse transcription (4, 6, 13, 14). TRIM5 proteins are composed of N-terminal RING, B-box 2, and coiled-coil domains. The C termini of TRIM5α and TRIM5CypA are the B30.2/SPRY and cyclophilin A (CypA) domains, respectively. All these domains in TRIM5 proteins are necessary to exert full restriction activity. Although the mechanism underlying TRIM5-mediated restriction has not been completely defined, inhibition of viral infection is initiated by capsid (CA) recognition with the

Received 7 June 2013 Accepted 9 August 2013
Published ahead of print 21 August 2013
Address correspondence to Hironori Sato, hirosato@nih.go.jp, or Akio Adachi, adachi@basic.med.tokushima-u.ac.jp.
M.N. and M.Y. contributed equally to this article.

doi:10.1128/JVI.01549-13

B30.2/SPRY or CypA domain. Sequence variation in the two domains determines species-specific restriction of retroviral infection. RhM *TRIM5* genes have been reported to be highly polymorphic (4, 6, 13, 14). Tetherin works as a virion release inhibition factor, and HIV-1 Vpu counteracts human but not macaque tetherin (4–6, 15). Tetherin may not be a potent barrier to limit cross-species transmission relative to APOBEC3G and TRIM5 proteins. However, tetherin antagonism is important for viral replication *in vivo*, because most primate lentiviruses have the ability to counteract tetherin, and tetherin-mediated restriction contributes to inhibiting viral replication *in vivo* (4, 5, 15). Recently, a novel anti-HIV-1 factor, SAMHD1, has been identified (4–6). Several Vpx and Vpr proteins appear to degrade SAMHD1 in a species-specific manner. However, SAMHD1 may be a weak species barrier, since HIV-1 has spread successfully and continuously in humans despite the lack of anti-SAMHD1 activity (4).

We and others have reported the construction of HIV-1 derivatives that have the ability to evade restriction factors for macaque model studies (16–21). As a common feature, all reported macaque-tropic HIV-1 (HIV-1mt) clones have the *vif* gene, which can neutralize macaque APOBEC3G (e.g., SIVmac239 *vif*). This modification is essential to evade APOBEC3G restriction and to gain the ability to replicate in macaque cells. To circumvent the restriction by TRIM5 proteins, two approaches have been taken. One approach is the use of pig-tailed macaques that do not express HIV-1-restrictive TRIM5 proteins. In this case, HIV-1 derivatives carrying authentic HIV-1 CA have been used as challenge viruses (stHIV-1_{SV} [16] and HSIV-vif [21]). Another approach is the replacement of the entire HIV-1 CA with the corresponding region of SIVmac239 (stHIV-1_{SCA+SV} [16, 17]). Although stHIV-1_{SCA+SV} replicates well in RhM cells, the CA region is not derived from HIV-1. Recently, chimeric viruses between simian-human immunodeficiency virus ($SHIV_{DH12}$ and $SHIV_{AD8}$) and an HIV-1 derivative (stHIV-1gsnU) that display anti-macaque tetherin activity have been reported (22, 23). However, the former construct is SHIV, and the latter is pig-tailed macaque-tropic HIV-1 carrying full-length SIVgsn71 (SIV from greater spot-nosed monkey) Vpu. While RhMs have been commonly and frequently used for viral infection experiments, no RhM-tropic HIV-1 derivatives that exhibit resistance to known major intrinsic restriction factors (APOBEC3, TRIM5, and tetherin proteins) have been reported.

We have previously described a unique HIV-1mt clone, designated MN4Rh-3, which can evade APOBEC3 and TRIM5CypA proteins but not TRIM5α and tetherin restrictions in macaque cells (Fig. 1) (19, 24). In this study, we generated new HIV-1mt clones from MN4Rh-3 that potentially possess an improved capacity to antagonize RhM TRIM5α and tetherin proteins. First, we constructed a number of MN4Rh-3 CA mutant clones; examined their growth potentials in an RhM lymphocyte cell line, M1.3S (25); and selected a new HIV-1mt clone, MN4/LSDQ, carrying only three amino acid substitutions in MN4Rh-3 CA (Fig. 1). MN4/LSDQ exhibited enhanced growth potential accompanied by increased resistance to macaque TRIM5α restriction. Next, we replaced the transmembrane (TM) domain of MN4/LSDQ Vpu with the corresponding region of SIVgsn166 (another SIVgsn) Vpu, which shows anti-macaque tetherin activity (26). The resultant clone, MN4/LSDQgtu, gained the ability to antagonize specifically macaque tetherin (Fig. 1). The replication efficiency of MN4/LSDQgtu in RhM peripheral blood mononuclear cells (PBMCs) was comparable to that of SIVmac239 and was

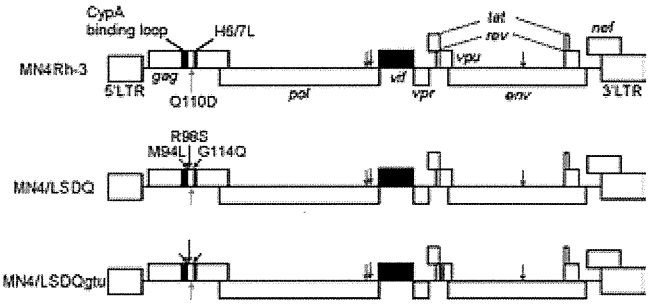

FIG 1 Proviral genome structures of various HIV-1mt clones. HIV-1 NL4-3 (32), SIVmac239 MA239 (71), and SIVgsn166 (GenBank accession number AF468659) sequences are indicated by white, black, and red areas, respectively. Green arrows show adaptive mutations that enhance viral growth potential (47). Orange arrows show the CA-Q110D mutation that augments viral growth in macaque cells/monkeys (19, 24). Blue arrows indicate CA substitutions (M94L/R98S/G114Q) identified in this study that are responsible for viral growth enhancement. H6/7L, loop between helices 6 and 7 in Gag-CA.

superior to those of the other HIV-1mt clones (MN4Rh-3 and MN4/LSDQ). MN4/LSDQgtu is the first HIV-1 derivative that is highly resistant to the known major restriction factors (APOBEC3, TRIM5, and tetherin proteins) in RhM cells. Generation of MN4/LSDQgtu also served to find amino acid residues in CA involved in the interaction with macaque TRIM5α and to verify HIV-1mt growth enhancement in macaque cells by macaque tetherin antagonism.

MATERIALS AND METHODS

Cells. An RhM lymphocyte cell line, M1.3S (25), was maintained in RPMI 1640 medium containing 10% heat-inactivated fetal bovine serum (FBS) and 50 units/ml of recombinant human interleukin-2 (IL-2) (Bio-Rad Laboratories Inc., Hercules, CA). The human monolayer cell lines 293T (27) and HEp2 (ATCC CCL-23) and the RhM kidney cell line LLC-MK2 (ATCC CCL-7) were maintained in Eagle's minimal essential medium (MEM) containing 10% FBS. MAGI cells (28) were cultured in MEM containing 10% FBS, 200 μg/ml G418 (Sigma-Aldrich Co., St. Louis, MO), and 100 μg/ml hygromycin B (Sigma-Aldrich Co.).

Plasmid DNA. The construction of MN4Rh-3, SIVmac239 clone MA239N, and its *nef*-deficient variant MA239N-ΔN was described previously (19, 25). CA alterations of HIV-1mt proviral clones were performed by replacing target sites of HIV-1mt CA with the corresponding sites of SIVmac239 (both codons and amino acids were changed to those of SIVmac239) by using the QuikChange site-directed mutagenesis kit (Agilent Technologies Inc., Santa Clara, CA). MN4/LSDQ was generated by introducing the following codon/amino acid substitutions into MN4Rh-3 (uppercase letters represent amino acids and lowercase letters represent codons): M(atg) to L(ctt) at amino acid position 94, R(agg) to S(tca) at position 98, and G(gga) to Q(cag) at position 114. Each *vpu* gene of SIVmon (SIV from mona monkey)/SIVmus (SIV from mustached monkey)/SIVgsn (SIVmon/mus/gsn) was synthesized (TaKaRa Bio Inc., Otsu, Japan) and cloned into pSG-cFLAG to express mon-, mus-, and gsn-Vpu, respectively, as described previously (29). Full-length Vpu sequences composed of the TM domain of SIVmon/mus/gsn Vpu and the cytoplasmic domain of HIV-1_{NL4-3} Vpu (monTM-, musTM-, and gsnTM-Vpu, respectively) were made by overlapping PCR and inserted into the pSG-cFLAG expression vector, as described previously (29). The resultant clones were designated pSG-VpucFLAG constructs. RhM and human tetherin sequences were amplified by PCR using cDNAs from M1.3S cells and HeLa cells, respectively. The amplified products were cloned into the pCIneo vector (Promega Corporation, Madison, WI) to generate pCIneo-RhM tetherin and pCIneo-Human tetherin. The sequence of RhM tetherin from M1.3S cells was identical to that of an RhM

tetherin variant [Mac(m)3] (30, 31). For flow cytometry analysis, pIRES-HIV-1-Vpu-hrGFP and pIRES-gsnTM-Vpu-hrGFP were constructed as described previously (29). The MN4/LSDQdtu clone was constructed by replacing the TM domain of MN4/LSDQ Vpu with the corresponding region of HIV-1_{DH12} Vpu (22) by using the QuikChange site-directed mutagenesis kit (Agilent Technologies Inc.). The MN4/LSDQgtu clone was generated by overlapping PCR between MN4/LSDQ and gsnTM-Vpu. *vpu*-deficient HIV-1mt clones were constructed by changing the initiation codon (ATG) to AGG and the second codon of each construct to TAG (stop codon).

Virus stocks and reverse transcriptase assay. Virus stocks were prepared from 293T cells transfected with proviral clones by the calcium-phosphate coprecipitation method (32). Virion-associated reverse transcriptase (RT) activity was measured as described previously (33), with the following modifications: 5 μl of culture supernatant was mixed with 25 μl of an RT reaction mixture containing a template primer of poly(A) (500 μg/ml; Midland Certified Reagent Company Inc., Midland, TX) and oligo$(dT)_{12-18}$ (1.25 μg/ml; New England BioLabs Inc., Ipswich, MA) in 50 mM Tris (pH 7.8), 75 mM KCl, 2 mM dithiothreitol, 5 mM $MgCl_2$, 0.05% Nonidet P-40, and 9.25 kBq of [α-^{32}P]dTTP (29.6 TBq/mmol; Perkin-Elmer Inc., Waltham, MA). After incubation at 37°C for 3 h, 10 μl of the reaction mixture was spotted onto DE81 anion-exchange paper (GE Healthcare UK Ltd., Buckinghamshire, England) and washed four times with 2× SSC (0.3 M NaCl plus 0.03 M sodium citrate) to remove unincorporated [α-^{32}P]dTTP. Spots were then counted with a scintillation counter.

Virus replication assays. Virus replication in M1.3S cells was monitored as described previously (25). For infection of macaque primary cells, RhM and CyM PBMCs were separated by Ficoll-Paque Plus (GE Healthcare UK Ltd.) and stimulated with RPMI 1640 medium containing 10% FBS, 50 units/ml of recombinant human IL-2, and 2 μg/ml of phytohemagglutinin L (PHA-L) (Roche Diagnostics GmbH, Mannheim, Germany). Primary PBMCs without $CD8^+$ cell depletion were used in this study. On day 3 poststimulation, cells were spin infected (34) with equal amounts of viruses prepared from transfected 293T cells and cultured in the presence of IL-2. Viral growth was monitored by RT activity released into the culture supernatants. The genotype of *TRIM5* alleles was analyzed as described previously (35).

TRIM5α susceptibility assays. Assays using recombinant Sendai virus (SeV)-RhM TRIM5α and SeV-CyM TRIM5α expression systems were performed as described previously (36). MT4 cells (10^5) were infected with SeV expressing each TRIM5α at a multiplicity of infection of 10 PFU per cell and incubated at 37°C for 9 h. Cells were then superinfected with HIV-1mt derivatives (20 ng of Gag-p24) or SIVmac239 (20 ng of Gag-p27). Culture supernatants were collected at intervals, and the amount of Gag-p24 or Gag-p27 produced was determined by using RETROtek antigen enzyme-linked immunosorbent assay (ELISA) kits (ZeptoMetrix Corporation, Buffalo, NY).

Virion release assays. Tetherin-null 293T cells were used for virion release assays. For analysis of Vpu expression vectors, subconfluent 293T cells in 24-well dishes were cotransfected with *vpu*-deficient MN4Rh-3 (300 ng), pCIneo-RhM tetherin (5 ng), and various pSG-VpucFLAG vectors (200 ng) by using Lipofectamine 2000 (Life Technologies Corporation, Carlsbad, CA). On day 2 posttransfection, virion production in the cell culture supernatants was measured by RT assays. For analysis of proviral clones, 700 ng of MA239N/MA239N-ΔN or 300 ng of MN4 derivatives and an appropriate amount of pCIneo-RhM tetherin or pCIneo-Human tetherin were used for cotransfection.

Flow cytometry analysis. Flow cytometry analysis was performed to examine cell surface CD4 or tetherin downregulation by Vpu, as described previously (29). For analysis of cell surface CD4, MAGI cells in 60-mm dishes were transfected with pIRES-hrGFP-Vpu vectors. On day 2 posttransfection, cells were trypsinized, washed with phosphate-buffered saline (PBS), and resuspended in PBS containing 10% FBS. Cells were then stained with a phycoerythrin (PE)-conjugated mouse anti-human CD4 antibody (BD Biosciences, San Jose, CA). For analysis of cell surface tetherin, LLC-MK2 or HEp2 cells in 60-mm dishes were transfected with pIRES-hrGFP-Vpu vectors and harvested as described above. Cells were then reacted with an anti-HM1.24 monoclonal antibody (a generous gift from Chugai Pharmaceutical Co. Ltd., Chuo-ku, Japan) and stained with a secondary PE-conjugated anti-mouse Ig antibody (BD Biosciences). Stained cells were analyzed with a FACSCalibur instrument using CELLQuest software (BD Biosciences).

Prediction of the effects of amino acid substitutions on the stability of the HIV-1mt CA N-terminal domain. The three-dimensional (3-D) model of the HIV-1mt CA N-terminal domain (NTD) was constructed by homology modeling using "MOE-Align" and "MOE-Homology" in the Molecular Operating Environment (MOE) (Chemical Computing Group Inc., Quebec, Canada) and refined as described previously (19). The crystal structure of the HIV-1 CA NTD at a resolution of 2.00 Å (Protein Data Bank [PDB] accession number 1M9C) (37) was used as the modeling template. The changes in the stability of the CA NTD by mutations were computed by using the Protein Design application in MOE. Single-point mutations on the CA protein were generated, and ensembles of protein conformations were generated by using the LowMode MD module in MOE to calculate average stability using Boltzmann distribution. Finally, the stability scores of the structures refined by energy minimization were obtained through the stability scoring function of the Protein Design application.

Structural modeling of the Vpu TM domains. We first constructed 3-D structural models for monomers of Vpu TM domains encoded in three HIV-1mt clones (MN4/LSDQ, MN4/LSDQdtu, and MN4/LSDQgtu) with PyMOL on the basis of the previously reported structure of the HIV-1_{BH10} Vpu TM domain (PDB accession number 1PI8) (38). The HIV-1_{BH10} Vpu TM domain has a sequence identical to that of the MN4/LSDQ Vpu TM domain. The 3-D structures of their tetramers were then predicted from the constructed monomer structures with Rosetta 3.4 (39). We performed symmetry docking and predicted 10,000 tetramer structures for each molecule. Among the predicted structures, the structure with the best total score was selected as the model of the respective molecules. We compared the predicted tetramer structure of the MN4/LSDQ Vpu TM domain with the nuclear magnetic resonance (NMR) structure of the tetramer of the HIV-1_{BH10} Vpu TM domain (PDB accession number 1PI8). Their overall structures were highly similar. The root mean square deviation of C-α atoms between them was 1.64 Å.

RESULTS

Sequence homology- and structure-based modifications led to the identification of HIV-1mt CA residues that are responsible for the enhancement of viral growth in RhM cells. TRIM5 proteins inhibit retroviral infection in a species-specific manner. The RhM *TRIM5* coding sequence is highly polymorphic, and common RhM *TRIM5* alleles (*Mamu-1* to *Mamu-7*) can be divided into three groups based on polymorphisms at amino acid positions 339 to 341 within the B30.2/SPRY domain: $TRIM5^{TFP}$ (*Mamu-1* to *Mamu-3*), $TRIM5^{Q}$ (*Mamu-4* to *Mamu-6*), and $TRIM5^{CypA}$ (*Mamu-7*) (35, 40, 41). CyM TRIM5α has a Q residue at the corresponding site ($TRIM5^{Q}$), and CyM TRIM5CypA has a CypA sequence slightly different from that of RhM TRIM5CypA (42, 43). RhM and CyM TRIM5α proteins encoded by $TRIM5^{TFP}$ and $TRIM5^{Q}$ inhibit HIV-1 infection. On the other hand, CyM TRIM5CypA, but not RhM TRIM5CypA, restricts HIV-1 replication (42, 43). We have shown previously that a CXCR4-tropic MN4Rh-3 clone evaded CyM TRIM5CypA but was susceptible to TRIM5α restriction (19) and that its replication in *TRIM5α* homozygous CyM PBMCs/individuals was strongly restricted (24). Similarly, MN4Rh-3 replicated quite well in a CyM HSC-F cell line ($TRIM5^{Q/CypA}$) but very poorly in an RhM M1.3S cell line

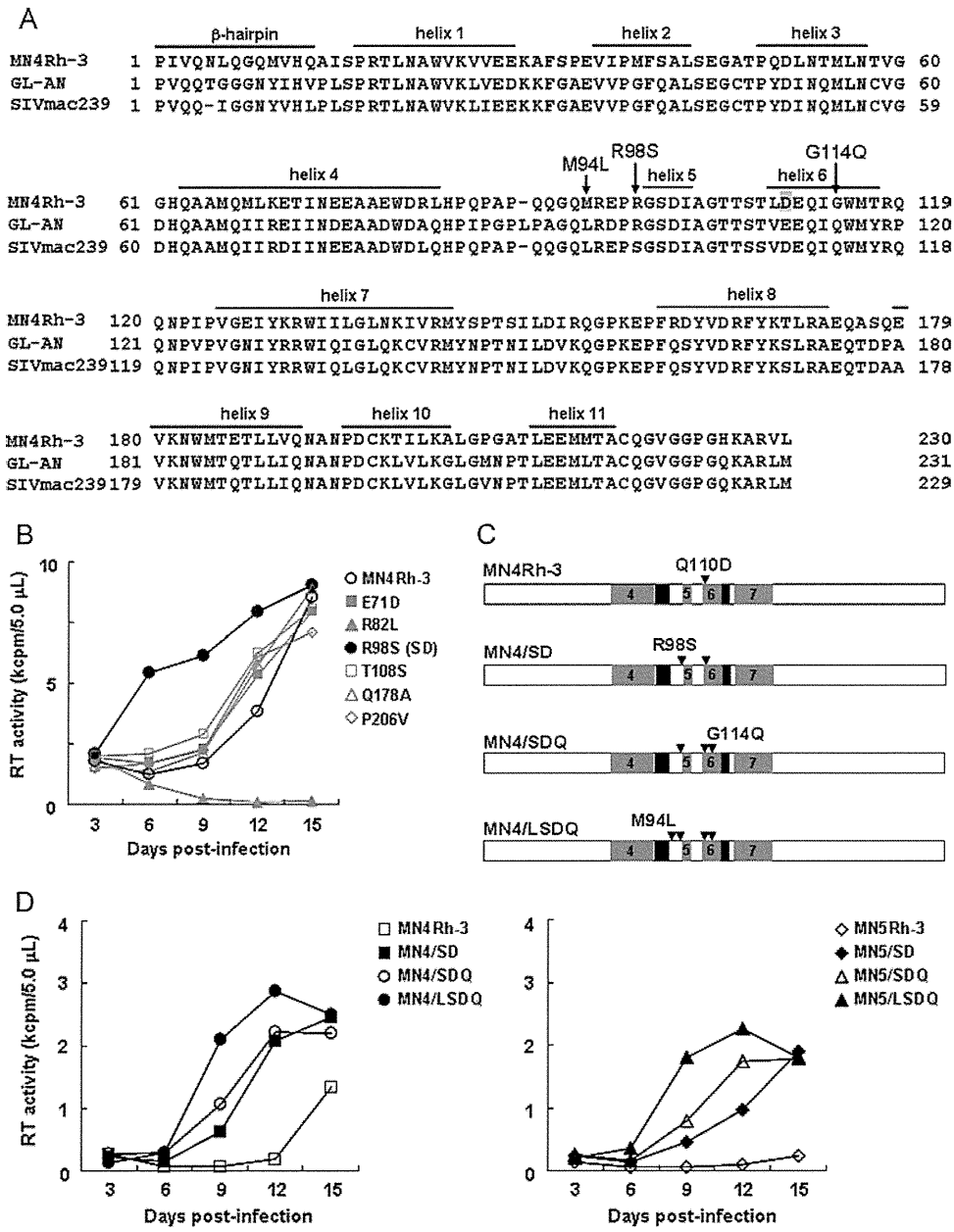

FIG 2 Identification of amino acid residues in HIV-1mt CA that are critical for viral growth enhancement in macaque cells. (A) Alignment of Gag-CA sequences. CA amino acid sequences of HIV-1mt MN4Rh-3 (19, 24), HIV-2 GL-AN (72), and SIVmac239 MA239 (71) are aligned. The N-terminal β-hairpin and helices 1 to 11 are indicated based on previously reported analyses (50, 73). The CA-Q110D mutation in MN4Rh-3 (19, 24) is shaded. Substitutions of three amino acids that contribute to the enhancement of HIV-1mt growth in macaque cells, described in this work, are indicated by arrows. (B) Growth kinetics of a parental clone, MN4Rh-3, and its CA mutants carrying a single-amino-acid change (see Table 1 for the mutants). Viruses were prepared from 293T cells transfected with the proviral clones indicated, and equal amounts (2×10^6 RT units) were inoculated into M1.3S cells (3×10^5 cells). Virus replication was monitored by RT activity released into the culture supernatants. Representative data from two independent experiments are shown. (C) Schematic CA structure of HIV-1mt clones. Amino acid substitutions are indicated in the order in which they were introduced into HIV-1mt CA. Black areas show sequences from SIVmac239. Helices 4 to 7 are shown as gray areas with the helix number. (D) Growth kinetics of CXCR4-tropic (left) and CCR5-tropic (right) HIV-1mt clones with different CA proteins (see reference 19 for CCR5-tropic MN5Rh-3). Viruses were prepared from 293T cells transfected with the indicated proviral clones, and equal amounts (2.5×10^6 RT units) were inoculated into M1.3S cells (10^6 cells). Virus replication was monitored by RT activity released into the culture supernatants. Representative data from two independent experiments are shown.

(*TRIM5*$^{TFP/TFP}$) (data not shown). Besides being a TRIM5α target, Gag-CA functions in various viral replication steps (44, 45). We thus used the M1.3S cell line as a target for multicycle infection to screen viral clones with increased replication potential following CA mutagenesis.

Modifications of MN4Rh-3 CA were performed based on sequence homology and structural modeling. As shown in Fig. 2A, the amino acid sequence identity of CA between HIV-1 and SIVmac239 is not high (~67% for SIVmac239 versus HIV-1_{NL4-3} and ~72% for SIVmac239 versus MN4Rh-3), but sequences are

relatively well conserved between HIV-2 and SIVmac239 (~90% for SIVmac239 versus HIV-2_{GL-AN}). Nevertheless, macaque TRIM5α restricts HIV-1 and HIV-2 infection but not SIVmac239. This distinct susceptibility to macaque TRIM5α results from the different CA sequences of each virus. We first selected amino acid residues in MN4Rh-3/HIV-2_{GL-AN} CA that are different from those of SIVmac239 CA and replaced these target residues with those of SIVmac239 (Table 1, MN4/SD and initial screening). The resultant clones were examined for their growth potential in M1.3S cells (Fig. 2B and Table 1). Of 25 clones tested, only MN4Rh-3 carrying an R98S change in CA (MN4/SD) exhibited enhanced viral growth efficiency (Table 1 and Fig. 2B). We previously found a growth-enhancing mutation, G114E, in CA by HIV-1mt adaptation in macaque cells (19). Since viral replication efficiency was decreased by the introduction of G114E into MN4Rh-3 (data not shown), we introduced an SIVmac239 CA-type G114Q mutation into the MN4/SD clone, and the resultant clone was designated MN4/SDQ (Fig. 2C and D). Moreover, we predicted an additional mutation that might improve the growth ability of MN4Rh-3 in macaque cells. Using HIV-2 CA, we previously found a key role of hydrogen bond formation between D97 within H4/5L (a loop between helices 4 and 5) and R119 within H6/7L (a loop between helices 6 and 7) in determining viral sensitivity to TRIM5α: TRIM5α-sensitive CA had a common H4/5L conformation with a decreased probability of hydrogen bond formation (46). The corresponding hydrogen bond was predicted to be formed between E96 in H4/5L and R118 in H6/7L of the MN4Rh-3 CA NTD. We assumed that the simultaneous introduction of SIV-CA-like amino acid residues at M94 in H4/5L and G114 in helix 6 might imitate the structural property of the SIVmac239 CA NTD surface for TRIM5α resistance and might be beneficial to improve the growth ability of MN4Rh-3 in macaque cells. The M94 residue is located in H4/5L, protruding its side chain near the G114 residue in helix 6. We therefore generated MN4/SDQ carrying the M94L mutation (MN4/LSDQ) (Fig. 2C and D). Three-dimensional locations of M94L, R98S, Q110D, and G114Q in the CA NTD are shown in Fig. 3. In addition, we constructed a series of CCR5-tropic viruses (MN5Rh-3, MN5/SD, MN5/SDQ, and MN5/LSDQ) (Fig. 2D), which carry the Env sequence derived from NF462 and a growth-enhancing Env S304G mutation (47). The growth potential of these viruses in M1.3S cells was analyzed. As shown in Fig. 2D, viral growth potential was enhanced with increasing amino acid substitutions in CA. MN4/LSDQ and MN5/LSDQ exhibited the highest replication potential in M1.3S cells in each group.

We constructed numerous HIV-1mt clones carrying CA mutations, including those described previously (48–50). All CA mutations and the growth potentials of the mutant viruses are summarized in Table 1. In the mutants derived from four HIV-1mt clones (MN4Rh-3, MN4/SD, MN4/SDQ, and MN4/LSDQ), most amino acid substitutions gave neutral or negative effects: CA amino acid substitutions that did not alter replication efficiency (L6I, E71D, T108S, Q178A, and P206V) or those that strikingly reduced the growth potential (e.g., Q50Y, T54Q, K70R, R82L, and L83Q; more than two consecutive mutations; and mutations in the β-hairpin domain). All listed HIV-1mt clones produced a significant amount of virions from transfected 293T cells, but none of them displayed a higher replication potential than MN4/LSDQ in M1.3S cells. In sum, M94L/R98S/G114Q substitutions in CA contributed to the growth enhancement of MN4Rh-3 in macaque cells.

Prediction of the effects of amino acid substitutions on the stability of the HIV-1 CA NTD. To investigate whether the M94L, R98S, Q110D, and G114Q mutations in MN4Rh-3 CA influenced the structural property of the protein, we analyzed the changes in stability by the mutations using the Protein Design application in MOE. The changes in stability by each of the point mutations M94L, R98S, Q110D, and G114Q were −0.41, 0.09, 0.25, and −1.70 kcal/mol, respectively (Fig. 3). The data suggested distinct effects of the single mutations at positions 94, 98, 110, and 114 on the stability of the HIV-1mt CA NTD. The Q110D mutation was predicted to destabilize the CA NTD. The R98S mutation has a similar negative effect on structure but to a much lesser extent. These mutations are considered to be more or less disadvantageous in terms of the CA structure. Nevertheless, they were critical for HIV-1mt growth enhancement in macaque cells (19) (Table 1 and Fig. 2). Therefore, these mutations must have given essential functions to CA protein in viral replication, which surpassed the structural disadvantage. On the other hand, M94L and G114Q mutations were predicted to stabilize the CA NTD. Therefore, these mutations may function as compensatory mutations that can redress structural disadvantages caused by R98S and Q110D mutations and increase growth ability in macaque cells. Our experimental data on MN4Rh-3, MN5Rh-3, and their derivatives having R98S/Q110D mutations, R98S/Q110D/G114Q mutations, and M94L/R98S/Q110D/G114Q mutations (Fig. 2) are consistent with this possibility.

Enhancement of viral replication efficiency by introduction of CA mutations (M94L/R98S/G114Q) correlates well with increased resistance to TRIM5α restriction. Some particular CA alterations (M94L/R98S/G114Q) of MN4Rh-3 markedly promoted viral replication in M1.3S cells with *TRIM5*$^{TFP/TFP}$ (Fig. 2D). Since TRIM5 proteins are potent restriction factors as species barriers (4, 8, 10) and can affect SIV transmission/replication *in vivo* (40, 51), it was expected that CA mutations (M94L/R98S/G114Q) would increase TRIM5α resistance as well as viral growth potential. To examine the effect of CA alterations on TRIM5α resistance, we carried out TRIM5α susceptibility assays using the recombinant SeV-TRIM5α expression system (36). TRIM5α resistance, as determined by this system, has been shown to be well reflected in the viral growth potential in macaque PBMCs/individuals due to the higher expression level of TRIM5α than that in feline CRFK cells stably expressing TRIM5α (19, 24). Four HIV-1mt clones (MN4Rh-3, MN4/SD, MN4/SDQ, and MN4/LSDQ) were assayed for their resistance to RhM-TRIM5α (*TRIM5*^{TFP}) and CyM-TRIM5α (*TRIM5*^{Q}), using SIVmac239 as a positive control. As shown in Fig. 4, the growth kinetics of SIVmac239 in cells expressing RhM- or CyM-TRIM5α or control B30.2/SPRY(−) TRIM5 were similar. Consistent with a previous analysis (19), MN4Rh-3 replication was strongly restricted in both RhM- and CyM-TRIM5α-expressing cells relative to that in control cells. Of note, TRIM5α resistance of MN4/SD, MN4/SDQ, and MN4/LSDQ quite paralleled their growth ability in M1.3S cells (see Fig. 2D for virus growth). While TRIM5α resistance of MN4/SD was increased relative to that of MN4Rh-3, MN4/SDQ exhibited higher resistance, especially to CyM-TRIM5α, than MN4/SD. MN4/LSDQ, which has the highest growth potential among the four HIV-1mt clones, showed the highest level of TRIM5α resistance, especially to RhM-TRIM5α. The HIV-1mt

TABLE 1 HIV-1mt CA mutants constructed in this study

Clone designation	CA mutation(s)[b]	Growth potential[c]
MN4Rh-3[a]	None (parental clone)	++
MN4/SD	R98S	+++
MN4/SDQ	R98S, G114Q	+++
MN4/LSDQ	M94L, R98S, G114Q	++++
Initial screening		
E71D	E71D	++
R82L	R82L	−
RL82LQ	RL82, 83LQ	−
T108S	T108S	++
Q178A	Q178A	++
P206V	P206V	++
PD	L6P	−
PDQ	L6P, G114Q	−
PYD	L6P, Q50Y	+
PYDQ	L6P, Q50Y, G114Q	+
PYQD	L6P, Q50Y, T54Q	+
PYQDQ	L6P, Q50Y, T54Q, G114Q	+
GG	LQ6, 7GG	−
GG-T117Y	LQ6, 7GG, T117Y	−
IGGN	LQGQ6-9IGGN	−
IGGN-T117Y	LQGQ6-9IGGN, T117Y	−
5IGGN	NLQGQ5-9IGGN	−
YD	Q50Y	−
YDQ	Q50Y, G114Q	−
YQD	Q50Y, T54Q	−
YQDQ	Q50Y, T54Q, G114Q	−
IIRDI	MLKET68-72IIRDI	−
TDA	ASQ176-178TDA	−
VNP	PGA206-208VNP	−
Mutants from MN4/SD		
L6I-S	L6I, R98S	++
YQ-S	Q50Y, T54Q, R98S	−
DS	E71D, R98S	+++
SS	R98S, T108S	+++
SA	R98S, Q178A	+++
SV	R98S, P206V	+++
SAV	R98S, Q178A, P206V	+++
DSAV	E71D, R98S, Q178A, P206V	+++
Mutants from MN4/SDQ or MN4/LSDQ		
L6I-LSDQ	L6I, M94L, R98S, G114Q	++++
YQ-LDQ	Q50Y, T54Q, M94L, G114Q	−
YQ-SDQ	Q50Y, T54Q, R98S, G114Q	−
YQ-LSDQ	Q50Y, T54Q, M94L, R98S, G114Q	−
K70R-LSDQ	K70R, M94L, R98S, G114Q	−
E71D-LSDQ	E71D, M94L, R98S, G114Q	+++
E79D-LSDQ	E79D, M94L, R98S, G114Q	++++
R82L-LSDQ	R82L, M94L, R98S, G114Q	−
L83Q-LSDQ	L83Q, M94L, R98S, G114Q	−
T108S-LSDQ	M94L, R98S, T108S, G114Q	++++
E79D-T108S-LSDQ	E79D, M94L, R98S, T108S, G114Q	++++
E127N-LSDQ	M94L, R98S, G114Q, E127N	+++
I134Q-LSDQ	M94L, R98S, G114Q, I134Q	−
LSDQN	M94L, R98S, G114Q, S148N	−
I152V-LSDQ	M94L, R98S, G114Q, I152V	+++
LSDQA	M94L, R98S, G114Q, Q178A	++++
IY-LSDQA	L6I, M10Y, M94L, R98S, G114Q, Q178A	++
YQ-LSDQA	Q50Y, T54Q, M94L, R98S, G114Q, Q178A	−
LSDQA-P159S	M94L, R98S, G114Q, P159S, Q178A	+++

(Continued on following page)

TABLE 1 (Continued)

Clone designation	CA mutation(s)[b]	Growth potential[c]
L6I-LSDQA	L6I, M94L, R98S, G114Q, Q178A	++++
DLSDQA	E71D, M94L, R98S, G114Q, Q178A	+++
L6I-DLSDQA	L6I, E71D, M94L, R98S, G114Q, Q178A	+++
LSDQAV	M94L, R98S, G114Q, Q178A, P206V	++++
L6I-LSDQAV	L6I, M94L, R98S, G114Q, Q178A, P206V	++++
YQ-LSDQAV	Q50Y, T54Q, M94L, R98S, G114Q, Q178A, P206V	−
DLSDQAV	E71D, M94L, R98S, G114Q, Q178A, P206V	+++
L6I-DLSDQAV	L6I, E71D, M94L, R98S, G114Q, Q178A, P206V	+++
Mutants of the β-hairpin domain		
DdN5	N5 deletion	−
DdN5-Y	N5 deletion, T117Y	−
SDdN5	N5 deletion, R98S	−
SDdN5-Y	N5 deletion, R98S, T117Y	−
DQdN5-Y	N5 deletion, G114Q, T117Y	−
SDQdN5	N5 deletion, R98S, G114Q	−
SDQdN5-Y	N5 deletion, R98S, G114Q, T117Y	−
LSDQdN5	N5 deletion, M94L, R98S, G114Q	−
LSDQdN5-Y	N5 deletion, M94L, R98S, G114Q, T117Y	−
QIG-S	NLQ5-7QIG, R98S	−
QIG-SDQ	NLQ5-7QIG, R98S, G114Q	−
QIG-LSDQ	NLQ5-7QIG, M94L, R98S, G114Q	−
GGN-S	QGQ7-9GGN, R98S	−
GGN-LSDQ	QGQ7-9GGN, M94L, R98S, G114Q	−
GGN-YQ-LSDQ	QGQ7-9GGN, Q50Y, T54Q, M94L, R98S, G114Q	−
L6I-YQ-LSDQ	L6I, Q50Y, T54Q, M94L, R98S, G114Q	−
IL-LSDQA	L6I, Q13L, M94L, R98S, G114Q, Q178A	−
IL-Y-LSDQA	L6I, Q13L, M94L, R98S, G114Q, T117Y, Q178A	−
IN-LSDQA	L6I, Q9N, M94L, R98S, G114Q, Q178A	−
IN-Y-LSDQA	L6I, Q9N, M94L, R98S, G114Q, T117Y, Q178A	−
IY-Y-LSDQA	L6I, M10Y, M94L, R98S, G114Q, T117Y, Q178A	−
INY-LSDQA	L6I, Q9N, M10Y, M94L, R98S, G114Q, Q178A	−
INY-Y-LSDQA	L6I, Q9N, M10Y, M94L, R98S, G114Q, T117Y, Q178A	−
INL-LSDQA	L6I, Q9N, Q13L, M94L, R98S, G114Q, Q178A	−
INL-Y-LSDQA	L6I, Q9N, Q13L, M94L, R98S, G114Q, T117Y, Q178A	−
IYL-LSDQA	L6I, M10Y, Q13L, M94L, R98S, G114Q, Q178A	−
IYL-Y-LSDQA	L6I, M10Y, Q13L, M94L, R98S, G114Q, T117Y, Q178A	−
INYL-LSDQA	L6I, Q9N, M10Y, Q13L, M94L, R98S, G114Q, Q178A	−
INYL-Y-LSDQA	L6I, Q9N, M10Y, Q13L, M94L, R98S, G114Q, T117Y, Q178A	−
Q13L-LSDQ	Q13L, M94L, R98S, G114Q	−
Q13L-Y-LSDQ	Q13L, M94L, R98S, G114Q, T117Y	−
Q13L-LSDQA	Q13L, M94L, R98S, G114Q, Q178A	−
Q13L-Y-LSDQA	Q13L, M94L, R98S, G114Q, T117Y, Q178A	−

[a] MN4Rh-3 CA was constructed by replacing the CypA-binding loop and H6/7L of HIV-1_{NL4-3} CA with the corresponding regions of SIVmac239 CA and by the additional introduction of a Q110D mutation (Fig. 1) (19, 24).

[b] Amino acid number in MN4Rh-3 CA.

[c] Viral growth potential in M1.3S cells. ++++, grows similarly to MN4/LSDQ; +++, grows more efficiently than MN4Rh-3; ++, grows similarly to MN4Rh-3; +, grows more poorly than MN4Rh-3; −, undetectable during the observation period.

clones here, except for MN4Rh-3, exhibited a tendency to have a higher level of resistance to CyM-TRIM5α than to RhM-TRIM5α (Fig. 4). It has been shown that TRIM5α proteins encoded by *TRIM5*^{TFP} are more restrictive to virus infection than are those encoded by *TRIM5*^{Q} (40). The observed tendency for TRIM5α resistance may be due to the difference between RhM-TRIM5α (*TRIM5*^{TFP}) and CyM-TRIM5α (*TRIM5*^{Q}) used in the assay. These results indicate that the enhancement of viral growth in M1.3S cells by CA alterations depends, at least in part, on the increased resistance to TRIM5α.

Virus replication capability in macaque PBMCs with different *TRIM5* alleles reflects the TRIM5α resistance of HIV-1mt clones. We have previously shown that MN4Rh-3 replicates well in *TRIM5α/TRIM5CypA* heterozygous CyM PBMCs/individuals, but its replication was restricted in *TRIM5α* homozygous CyM PBMCs/individuals (19, 24). To confirm the effect of the increased resistance of MN4/LSDQ and MN5/LSDQ against macaque TRIM5α on viral replication, we examined their replication potential relative to that of MN4Rh-3 and MN5Rh-3 in *TRIM5α/TRIM5CypA* heterozygous or *TRIM5α* homozygous macaque PBMCs.

First, we compared viral growth potentials of the clones in CyM PBMCs (Fig. 5A). Growth kinetics of MN4Rh-3 and MN4/LSDQ were similar in *TRIM5α/TRIM5CypA* heterozygous CyM

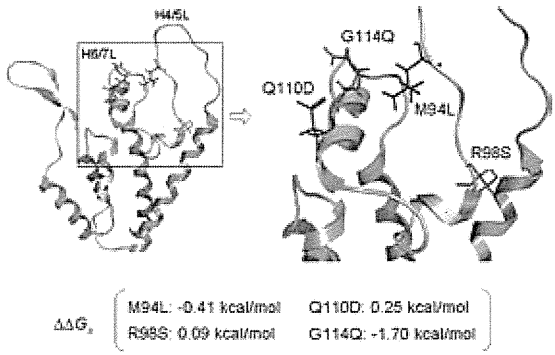

FIG 3 Structural analysis of the HIV-1mt CA NTD. A molecular model of the HIV-1mt CA NTD was constructed by homology modeling and refined as described previously (19). Single-point mutations were generated on the CA model, and ensembles of protein conformations were generated by using the LowMode MD module in MOE (Chemical Computing Group Inc., Quebec, Canada) to calculate average stability by using Boltzmann distribution. The stability scores ($\Delta\Delta G_s$) of the structures refined by energy minimization were obtained through the stability scoring function of the Protein Design application and are indicated below the structural model.

PBMCs. In contrast, the replication efficiency of MN4/LSDQ was markedly enhanced in *TRIM5α* homozygous CyM PBMCs relative to that of MN4Rh-3 (Fig. 5A). Similar results were obtained with RhM PBMCs. MN4Rh-3 exhibited growth kinetics comparable to those of MN4/LSDQ in *TRIM5α*/*TRIM5CypA* heterozygous RhM PBMCs (Fig. 5B). In *TRIM5α* homozygous RhM PBMCs, MN5/LSDQ replicated much more efficiently than MN5Rh-3 (Fig. 5C). CXCR4-tropic HIV-1mt clones (MN4 series) were found to exhibit a higher growth ability than CCR5-tropic HIV-1mt clones (MN5 series) in both M1.3S cells and macaque PBMCs (Fig. 2D and 5B and C) and were therefore used for experiments thereafter. In sum, the replication potential of TRIM5α-resistant HIV-1mt clones (MN4/LSDQ and MN5/LSDQ) markedly increased in *TRIM5α* homozygous PBMCs but was similar to that of TRIM5CypA-resistant/TRIM5α-sensitive clones (MN4Rh-3 and MN5Rh-3) in *TRIM5α*/*TRIM5CypA* heterozygous PBMCs. These results suggest that M94L/R98S/G114Q mutations in MN4Rh-3 CA largely contribute to the acquisition of TRIM5α resistance.

HIV-1 Vpu gains the ability to specifically counteract macaque tetherin by replacing its TM domain with the corresponding region of SIVgsn166 Vpu. Tetherin as well as TRIM5 proteins are important anti-HIV-1 factors in macaque cells (4, 8, 10), but the HIV-1mt clones constructed so far do not display macaque tetherin antagonism due to Vpu derived from HIV-1_{NL4-3}. It has been shown that Vpu from SIVmon/mus/gsn can antagonize macaque tetherin but not human tetherin (26). To confer the ability to counteract macaque tetherin on HIV-1mt clones, we modified the *vpu* gene. The sequence of the cytoplasmic domain of HIV-1 Vpu partially overlaps the 5′-end sequence of Env, and the TM domain of Vpu is a key region for species-specific tetherin antagonism (22). Thus, we constructed Vpu clones that contain SIVmon/mus/gsn TM and HIV-1mt cytoplasmic domains (Fig. 6A). First, RhM tetherin antagonism of various Vpu clones was analyzed by Vpu *trans*-complementation assays for virion release (Fig. 6B). 293T cells were cotransfected with a *vpu*-deficient HIV-1mt clone (MN4Rh-3-ΔU), an RhM tetherin expression vector (pCIneo-RhM tetherin), and various Vpu constructs, and virion production from cells on day 2 posttransfection was measured. While MN4Rh-3-ΔU released progeny virions efficiently upon transfection without RhM tetherin expression, its virion production was significantly inhibited in the presence of RhM tetherin. Although this reduction was not rescued by HIV-1_{NL4-3} Vpu, SIVmon/mus/gsn Vpu restored it to some extent, consistent with a previous report (26). Of the SIV/HIV-1 chimeric Vpu proteins, gsnTM-Vpu appeared to be somewhat better than the others and was therefore used thereafter.

Next, we examined the ability of HIV-1_{NL4-3} Vpu and gsnTM-Vpu to downregulate cell surface CD4 and tetherin (Fig. 6C). MAGI, LLC-MK2, and HEp2 cells were used for analysis of CD4,

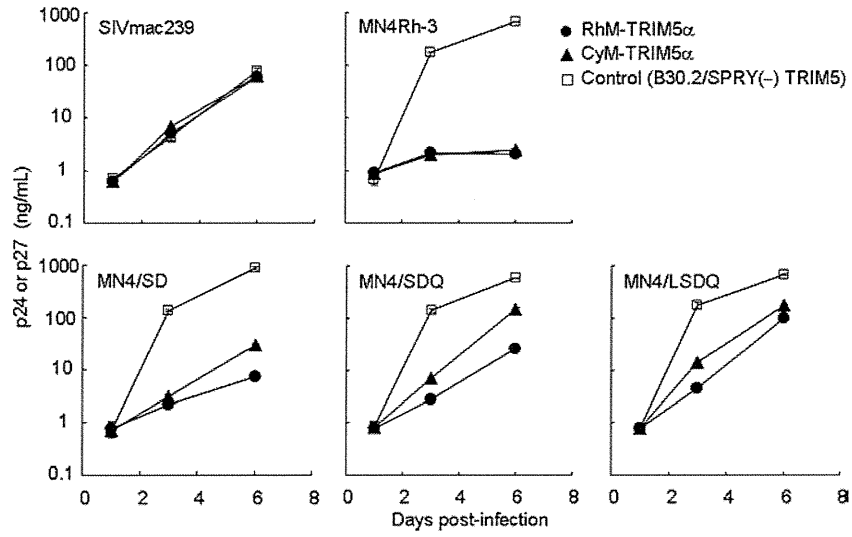

FIG 4 Susceptibility of SIVmac239 and various HIV-1mt clones to macaque TRIM5α. Human MT4 cells (10^5) were infected with recombinant SeV expressing RhM-TRIM5α (*TRIM5*^{TFP}), CyM-TRIM5α (*TRIM5*^{Q}), or B30.2/SPRY(−) TRIM5. Nine hours after infection, cells were superinfected with 20 ng (Gag-p24) of various HIV-1mt clones or 20 ng (Gag-p27) of SIVmac239. Virus replication was monitored by the amount of Gag-p24 from HIV-1mt clones or Gag-p27 from SIVmac239 in the culture supernatants. Error bars show actual fluctuations between duplicate samples. Representative data from two independent experiments are shown.

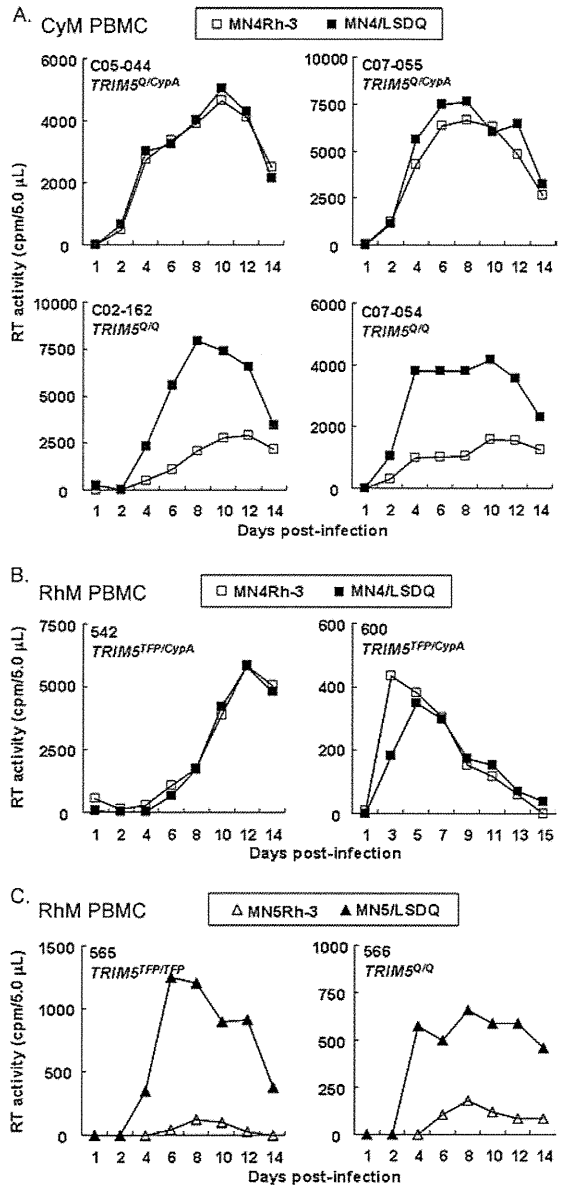

FIG 5 Growth kinetics of HIV-1mt clones with a distinct CA in macaque PBMCs. (A) Infection of PBMCs from four *TRIM5α/TRIM5CypA* heterozygous or *TRIM5α* homozygous CyM individuals. (B and C) Infection of PBMCs from four RhM individuals with different *TRIM5* alleles. For infection, input viruses were prepared from 293T cells transfected with the proviral clones indicated, and equal amounts (2.5×10^6 RT units) were used to spin infect PBMCs (2×10^6 cells). Virus replication was monitored by RT activity released into the culture supernatants. Monkey identification numbers are indicated in each panel.

RhM tetherin, and human tetherin, respectively. Cells were transfected with Vpu-green fluorescent protein (GFP) bicistronic expression plasmids and subjected to flow cytometry analysis on day 2 posttransfection. While both HIV-1_{NL4-3} Vpu and gsnTM-Vpu significantly decreased cell surface CD4 levels, the RhM tetherin level was reduced by gsnTM-Vpu but not by HIV-1_{NL4-3} Vpu. Similar results were obtained for MK.P3(F) cells expressing endogenous CyM tetherin (data not shown). In contrast, HIV-1_{NL4-3} Vpu but not gsnTM-Vpu downmodulated cell surface human tetherin. These results show that the transfer of the SIVgsn166 Vpu TM domain to HIV-1 Vpu is sufficient to confer the ability to specifically antagonize macaque tetherin on viruses.

gsnTM-Vpu in the context of proviral genome functions in macaque cells. To ask if gsnTM-Vpu is functional in the proviral context, we generated an HIV-1mt clone encoding gsnTM-Vpu (MN4/LSDQgtu) (Fig. 1 and 7A). Interestingly, it has been shown that Vpu of HIV-1 composed of HIV-1_{DH12} TM and HIV-1_{NL4-3} cytoplasmic domains counteracts macaque tetherin (22). We thus constructed another HIV-1mt clone, MN4/LSDQdtu, that has chimeric Vpu, as described above (Fig. 7A).

To examine the species-specific tetherin antagonism of these proviral clones, we carried out virion release assays in the presence of RhM or human tetherin (Fig. 7B). Using SIVmac239 Nef as a control antagonist against macaque tetherin (52, 53), the anti-macaque tetherin activities of MN4/LSDQ, MN4/LSDQdtu, and MN4/LSDQgtu were comparatively analyzed. As described above, SIVmac239 Nef exhibited the ability to specifically antagonize macaque tetherin. As expected, virion production of MN4/LSDQ and its *vpu*-deficient clone was similarly restricted in the presence of RhM tetherin, and MN4/LSDQ displayed a higher level of virion production than that of its *vpu*-deficient clone in the presence of human tetherin, indicating its specific antagonism to human tetherin. Also, as expected from a previous report (22), MN4/LSDQdtu showed both RhM and human tetherin antagonism, although its anti-RhM tetherin activity was relatively low. Strikingly, virion production levels of MN4/LSDQgtu in the presence of RhM/human tetherin were similar to those of SIVmac239. This indicates that MN4/LSDQgtu has specifically strong anti-RhM tetherin activity, as is the case for SIVmac239. To see if various Vpu proteins function during viral replication in macaque cells, we determined the growth properties of various HIV-1mt clones carrying distinct Vpu proteins. Although the effect of *vpu* deletion is virologically small, *vpu*-deficient viruses are readily distinguishable from the parental wild-type virus by comparative kinetic analysis of viral growth (22, 29). As shown in Fig. 7C, while MN4/LSDQ and MN4/LSDQdtu exhibited growth kinetics similar to those of their respective *vpu*-deficient clones, *vpu*-deficient MN4/LSDQgtu grew significantly more poorly than its parental virus. Taken together, it can be concluded that MN4/LSDQgtu Vpu but not MN4/LSDQ Vpu functions during viral replication in M1.3S cells. However, the functionality of MN4/LSDQdtu Vpu in macaque cells was not clear in the viral growth kinetics here. Although there are some possible explanations, the relatively low anti-RhM tetherin activity of MN4/LSDQdtu (see the results in Fig. 7B) could account for this observation.

Although the tertiary structure of the HIV-1 Vpu TM domain has been determined by NMR (38), the structure of the TM domain from SIV Vpu has not been solved to date. To investigate how replacement of the Vpu TM domain could lead to changes in TM structure, we constructed structural models of Vpu TM domains of MN4/LSDQ, MN4/LSDQdtu, and MN4/LSDQgtu (Fig. 7D). This modeling study revealed that the types of amino acid residues corresponding to the crucial residues (54) in HIV-1 Vpu for binding with human tetherin are similar between MN4/LSDQ and MN4/LSDQdtu, whereas they are often different in MN4/LSDQgtu. In addition, their steric locations in the helices are also similar between MN4/LSDQ and MN4/LSDQdtu, whereas they are very different in MN4/LSDQgtu. Finally, angles between the

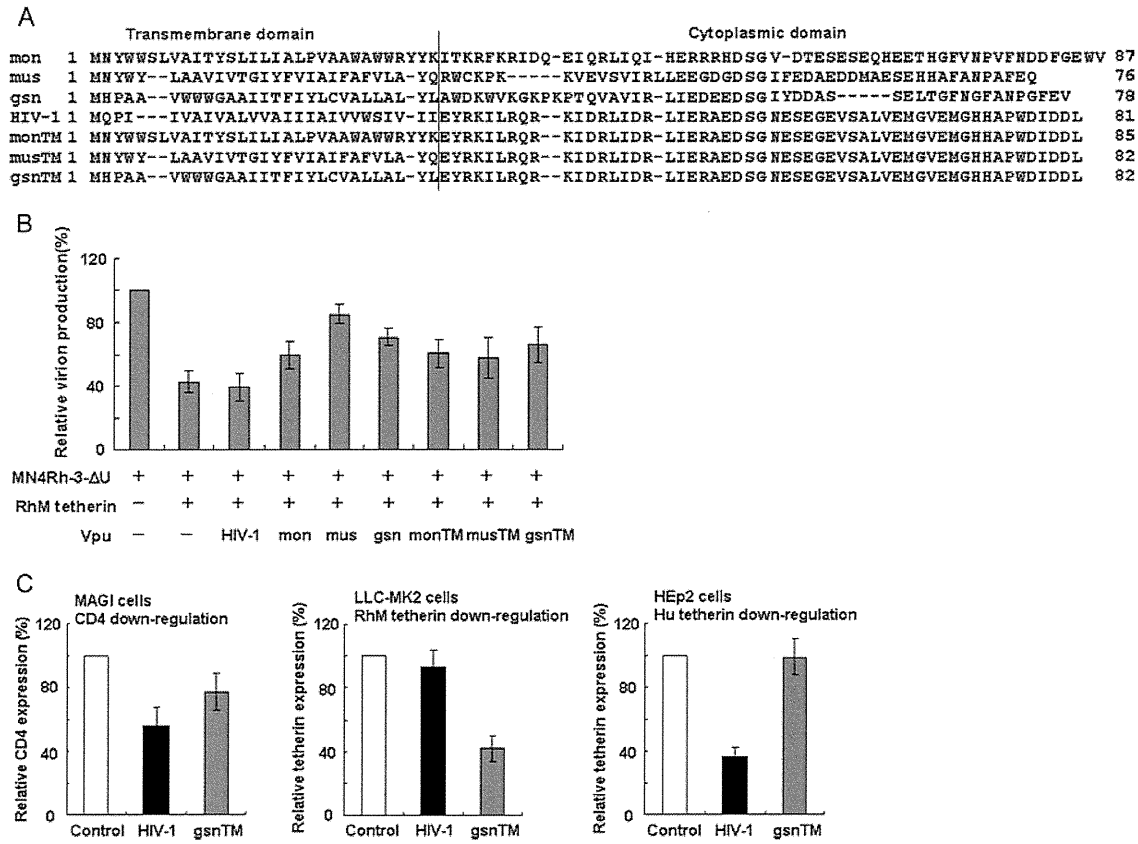

FIG 6 Generation of SIV/HIV-1 chimeric Vpu proteins resistant to macaque tetherin. (A) Amino acid sequences of various Vpu proteins. Alignments of the sequences and the boundary between TM/cytoplasmic domains are shown based on previously reported information (26). mon, SIVmonCML1 (GenBank accession number AY340701); mus, SIVmus1085 (GenBank accession number AY340700); gsn, SIVgsn166 (GenBank accession number AF468659); HIV-1, NL4-3 (32). HIV-1mt clones (MN4 series) have *vpu* genes identical to that of NL4-3. monTM-, musTM-, and gsnTM-Vpu were constructed by fusing each TM domain of SIVmon/mus/gsn Vpu with the cytoplasmic domain of HIV-1_{NL4-3} Vpu. (B) RhM tetherin antagonism by various Vpu proteins. 293T cells were cotransfected with a *vpu*-deficient proviral clone (MN4Rh-3-ΔU), pCIneo-RhM tetherin, and various pSG-VpucFLAG constructs. On day 2 posttransfection, virion production in the culture supernatants was determined by RT assays. Virion production levels relative to that of MN4Rh-3-ΔU in the absence of RhM tetherin were calculated, and mean values of three independent experiments are shown with the standard deviations. (C) Downregulation of cell surface CD4 and tetherin by HIV-1_{NL4-3} Vpu or gsnTM-Vpu. MAGI, LLC-MK2, and HEp2 cells were used to determine the downregulation of CD4, RhM tetherin, and human (Hu) tetherin by Vpu, respectively. Cells were transfected with the pIRES-hrGFP (control), pIRES-HIV-1 Vpu-hrGFP, or pIRES-gsnTM-Vpu-hrGFP construct. On day 2 posttransfection, cells were stained for cell surface CD4 or tetherin and analyzed by two-color flow cytometry. Values presented are CD4 or tetherin fluorescence intensities of GFP-positive cells relative to that of the control. Mean values ± standard deviations of three independent experiments are shown.

central lines of the helices are similar between MN4/LSDQ and MN4/LSDQdtu, whereas they are different in MN4/LSDQgtu. These results suggest the possibility that the structural properties of the tetherin interaction surface of the MN4/LSDQgtu Vpu TM domain are very different from those of the Vpu TM domains of MN4/LSDQ and MN4/LSDQdtu. Further studies are necessary to verify this issue.

RhM APOBEC3-, TRIM5α-, and tetherin-resistant HIV-1mt clone MN4/LSDQgtu replicates comparably to SIVmac239 in RhM PBMCs. Here we constructed distinct HIV-1mt clones with respect to their resistance to RhM TRIM5α and tetherin: TRIM5α- and tetherin-susceptible MN4Rh-3, TRIM5α-resistant but tetherin-susceptible MN4/LSDQ, and TRIM5α- and tetherin-resistant MN4/LSDQgtu. Of note, all these clones are RhM APOBEC3 resistant (see Fig. 1 for their genomes). To investigate the effect of the increased resistance to these macaque restriction factors, various viruses were examined for their growth potential in PBMCs from four *TRIM5α* homozygous RhM individuals. As shown in Fig. 8, SIVmac239, a comparative standard virus in macaque cells, replicated constantly in all PBMC preparations. The growth potentials in the RhM PBMCs of the HIV-1mt clones tested markedly and stably differed. As a likely result of RhM TRIM5α-resistant Gag-CA, MN4/LSDQ replicated much more efficiently than MN4Rh-3. By virtue of RhM tetherin-resistant Vpu, MN4/LSDQgtu grew significantly better than MN4/LSDQ. Essentially the same results for HIV-1mt growth kinetics were obtained in M1.3S cells. The M1.3S cell line and macaque PBMCs always responded similarly to various SIVs/HIVs (our unpublished observations). Moreover, by comparing the peak day of viral growth kinetics and the peak level itself, MN4/LSDQgtu was shown here to have the ability to replicate comparably to SIVmac239 in RhM PBMCs, except for one preparation (from monkey 565) (Fig. 8). The results show that the increased resistance to macaque restriction factors correlates well with the enhanced viral growth potential. In sum, MN4/LSDQgtu, which exhibits resistance to known major restriction factors (APOBEC3, TRIM5, and tetherin

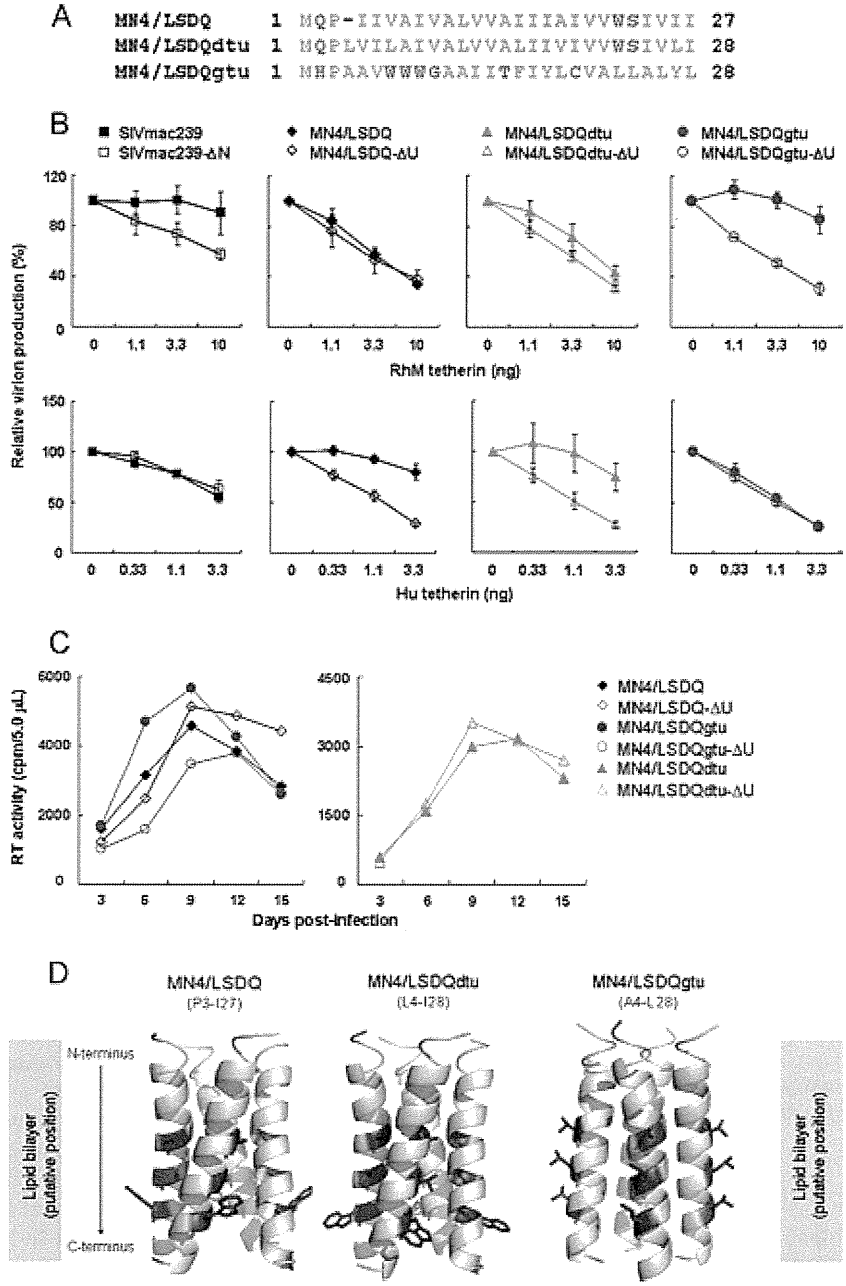

FIG 7 Effects of various Vpu proteins carrying a different TM domain on tetherin antagonism and HIV-1mt replication in macaque cells. (A) Alignment of amino acid sequences of the Vpu TM domain in each HIV-1mt clone. MN4/LSDQ, MN4/LSDQdtu, and MN4/LSDQgtu encode the Vpu TM domain derived from HIV-1_{NL4-3} (32), HIV-1_{DH12} (22), and SIVgsn166 (GenBank accession number AF468659), respectively. (B) Species-specific tetherin antagonism by SIVmac239 and various HIV-1mt clones carrying different Vpu proteins. SIVmac239 (MA239N) and its *nef*-deficient clone (MA239N-ΔN) were used as positive controls for RhM tetherin resistance. 293T cells were cotransfected with proviral clones and the indicated amounts of the pCIneo-RhM tetherin or pCIneo-Human tetherin expression vector. On day 2 posttransfection, virion production was determined by RT activity released into the culture supernatants. Values are presented as RT activity of each sample relative to that of each proviral clone without tetherin expression. Mean values ± standard deviations of three independent experiments are shown. ΔU, *vpu* deficient; Hu, human. (C) Growth kinetics of various HIV-1mt clones and their *vpu*-deficient clones in M1.3S cells. Viruses were prepared from 293T cells transfected with the indicated proviral clones, and equal amounts (5×10^5 RT units) were inoculated into M1.3S cells (2×10^5 cells). Virus replication was monitored by RT activity released into the culture supernatants. Representative data from three independent experiments are shown. (D) Structural modeling of Vpu TM domains of MN4/LSDQ, MN4/LSDQdtu, and MN4/LSDQgtu. Predicted models are shown in a ribbon representation. Amino acid residues corresponding to the residues in HIV-1 Vpu crucial for binding with human tetherin (54) are highlighted in a red stick representation. Crucial residues in Vpu TM domains of MN4/LSDQ, MN4/LSDQdtu, and MN4/LSDQgtu are A14/A18/W22, A15/V19/W23, and T15/L19/L23, respectively. TM regions analyzed (see panel A for amino acid sequences) are indicated in parentheses.

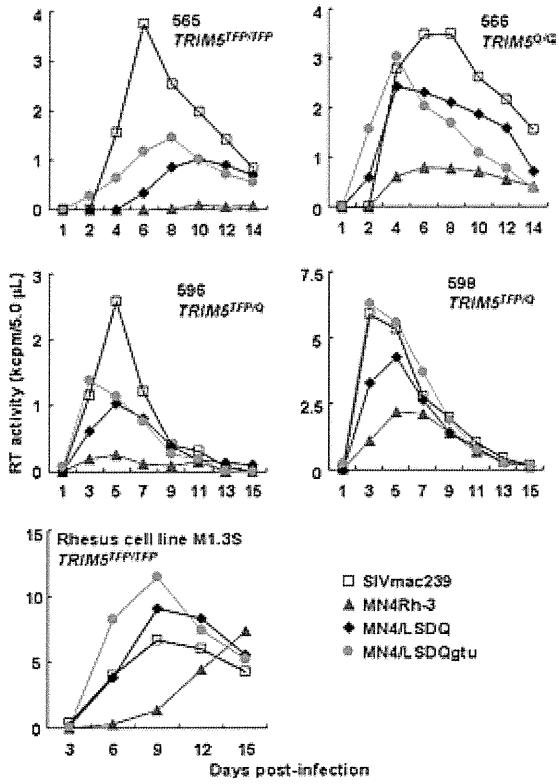

FIG 8 Growth kinetics of SIVmac239 and various HIV-1mt clones in *TRIM5α* homozygous RhM PBMCs. PBMCs were prepared from four RhM individuals with the different *TRIM5* alleles indicated. Viruses were prepared from 293T cells transfected with the indicated proviral clones, and equal amounts (2.5×10^6 RT units) were used to spin infect PBMCs (2×10^6 cells). As a control experiment, rhesus M1.3S cells (2×10^5) were infected with equal amounts of viruses (5×10^5 RT units). Virus replication was monitored by RT activity released into the culture supernatants. Monkey identification numbers are indicated in each panel.

proteins), is the best HIV-1mt clone generated so far, replicating with an efficiency similar to that of SIVmac239 in RhM cells.

DISCUSSION

In this study, we generated a novel HIV-1mt clone, designated MN4/LSDQgtu, that exhibits resistance to RhM TRIM5α and tetherin in addition to APOBEC3 proteins (Fig. 1). By sequence homology- and structure-guided CA mutagenesis and by screening the multicycle growth potential of CA mutant viruses in M1.3S cells, we successfully obtained viruses with enhanced replication efficiency in macaque cells as well as increased macaque TRIM5α resistance (Fig. 2 to 5). The transfer of the TM domain of SIVgsn166 Vpu into the corresponding region of HIV-1mt Vpu conferred the ability to specifically counteract macaque tetherin on the virus (Fig. 6 and 7). Furthermore, the increased resistance to both RhM TRIM5α and tetherin contributed to the viral growth enhancement in RhM PBMCs (Fig. 8).

During the preparation of this paper, McCarthy et al. reported several key residues in SIVmac239 CA involved in the interaction with RhM TRIM5α by genetic and structural analysis (55). Interestingly, the HIV-1mt CA amino acid residues identified in this study as being the elements responsible for the increased resistance to RhM TRIM5α (M94L/R98S/Q110D/G114Q) were included in those residues. McCarthy et al. reported that H4/5L and helix 6 of SIVmac239 CA also affect TRIM5α sensitivity (55). In the construction process for our HIV-1mt clones, we found that the CA elements involved in the interaction with RhM TRIM5α are the CypA-binding loop within H4/5L, H6/7L, M94L/R98S within H4/5L, and Q110D/G114Q in helix 6 (18–20, 56; this study). Of the substitutions identified in this study, R98S was the primary residue to increase TRIM5α resistance and improve viral growth in macaque cells. It was also shown that the TRIM5α ($TRIM5^{TFP}$)-susceptible SIVsmE543-3 clone acquires an adaptive R97S change in CA (corresponding to R98S in MN4Rh-3 CA) to evade TRIM5α ($TRIM5^{TFP}$) restriction during viral replication in RhM individuals (40). In TRIM5α-sensitive CA, R98S may be a key residue contributing to the evasion of TRIM5α restriction. Together, these results suggest that CA elements critical for recognition by TRIM5α may be conserved among primate lentiviruses. The RhM TRIM5α-resistant HIV-1 CA constructed in this study would be useful to define how TRIM5α recognizes CA. On the other hand, MN4/LSDQ appeared not to evade TRIM5α restriction completely, as SIVmac239 did (Fig. 4). In this regard, since it has been shown that the N-terminal β-hairpin domain in the retroviral CA contributes to circumventing TRIM5α (36, 55, 57), we constructed various HIV-1mt clones carrying mutations in the domain (Table 1). However, except for the L6I substitution, none of the clones were infectious (Table 1). A further CA modification(s) may be necessary for complete evasion of TRIM5α restriction.

Accumulating evidence has shown that tetherin is an important cellular restriction factor that affects the replication, adaptation, and evolution of primate immunodeficiency viruses (4, 26). Its negative effect on viral replication is certainly observed in cultured cell lines and primary cells but is not so evident relative to those of APOBEC3 and TRIM5 proteins (10). Also, in the present study, RhM tetherin-resistant Vpu significantly contributed to viral growth enhancement but not as much as TRIM5α-resistant CA (Fig. 7 and 8). However, tetherin has been suggested to play an important effector role in antiretroviral activity induced by alpha interferon (58–60). Also, it has been shown that the pathogenic revertant virus from nonpathogenic *nef*-deficient virus acquires tetherin antagonism by adaptive mutations in the gp41 subunit of Env (61). Therefore, the ability of HIV-1mt clones to antagonize RhM tetherin may be very important for optimal replication and pathogenesis in RhM individuals. In this regard, it has been described that naturally occurring polymorphisms in RhM tetherin sequences are present (30, 31, 61). Although whether these variations have some appreciable effects on viral replication *in vitro* is undetermined, the relationship between tetherin polymorphisms and the viral replication level *in vivo* (animals)/viral pathogenic activity *in vivo* may be a major issue to address and remains to be extensively analyzed. It would be intriguing to elucidate how the viral accessory protein Vpu *in vitro* is associated with the *in vivo* replicative and pathogenic properties of HIV-1 (22).

We constructed an MN4/LSDQgtu clone resistant to the known major restriction factors (APOBEC3, TRIM5, and tetherin proteins) in RhM cells. The growth potential of MN4/LSDQgtu was similar to that of SIVmac239 in most RhM PBMC preparations (Fig. 8). It was shown previously that the *in vivo* replication of SIV is predictable from the virus susceptibility of PBMCs (62, 63). Also, in a series of our studies, the better our HIV-1mt clones grew in PBMCs, the better they grew in the monkeys (20, 24, 64).

Thus, it is expected that MN4/LSDQgtu will grow much better in RhM individuals, at least in the early infection phase, than the other HIV-1mt clones constructed. As reported previously, the replication of HIV-1 derivatives in infected macaques was eventually controlled, and no disease was induced in the animals (16, 20, 21, 24, 64). It has been suggested that the replication ability of primate lentiviruses in unusual hosts is more severely affected, via an interferon-induced antiviral state mediated by unidentified species-specific factors, than that in natural hosts (23). Moreover, there are the other significant issues to be considered, such as viral coreceptor tropism (CXCR4 versus CCR5), the diversity in viral growth properties (HIV-1 versus SIVmac), and the difference in host immune responses (human versus RhM) (9, 65–67). Most importantly, CCR5-tropic but not CXCR4-tropic clones have been found to be appropriate as input viruses to experimentally infect RhMs for various HIV-1 model studies *in vivo* (65–67). Although MN4/LSDQgtu is a CXCR4-tropic virus, it has clear potential for the establishment of a model system. MN4/LSDQgtu can be changed to a pathogenic CCR5-tropic virus through *in vitro* and *in vivo* approaches, as well documented by previous SHIV studies (68–70). It is also possible to generate entirely new CCR5-tropic HIV-1mt clones other than MN4/LSDQgtu derivatives on the basis of the key findings for Gag-CA and Vpu-TM in this study.

Our study here describes the generation and characterization of a novel HIV-1 derivative minimally chimeric with SIVs. Several infection model systems using distinct viruses and nonhuman primates are now available. It is important to define common and unique characteristics of each virus-host interaction based on the results obtained from various experimental approaches, including SIV/natural host and SIVmac/RhM, SHIV/RhM, and HIV-1mt/RhM infection systems. Such efforts would shed light on a better understanding of HIV-1/human infection and HIV-1 pathogenesis.

ACKNOWLEDGMENTS

This study was supported in part by a grant from the Ministry of Health, Labor and Welfare of Japan (Research on HIV/AIDS project no. H23-003).

We thank Kazuko Yoshida for editorial assistance.

We declare that no competing interests exist.

REFERENCES

1. **Kirchhoff F.** 2010. Immune evasion and counteraction of restriction factors by HIV-1 and other primate lentiviruses. Cell Host Microbe **8**:55–67.
2. **Sharp PM, Hahn BH.** 2011. Origins of HIV and the AIDS pandemic. Cold Spring Harb. Perspect. Med. **1**:a006841. doi:10.1101/cshperspect.a006841.
3. **Shibata R, Sakai H, Kawamura M, Tokunaga K, Adachi A.** 1995. Early replication block of human immunodeficiency virus type 1 in monkey cells. J. Gen. Virol. **76**:2723–2730.
4. **Blanco-Melo D, Venkatesh S, Bieniasz PD.** 2012. Intrinsic cellular defenses against human immunodeficiency viruses. Immunity **37**:399–411.
5. **Harris RS, Hultquist JF, Evans DT.** 2012. The restriction factors of human immunodeficiency virus. J. Biol. Chem. **287**:40875–40883.
6. **Malim MH, Bieniasz PD.** 2012. HIV restriction factors and mechanisms of evasion. Cold Spring Harb. Perspect. Med. **2**:a006940. doi:10.1101/cshperspect.a006940.
7. **Hatziioannou T, Evans DT.** 2012. Animal models for HIV/AIDS research. Nat. Rev. Microbiol. **10**:852–867.
8. **Nomaguchi M, Doi N, Fujiwara S, Adachi A.** 2011. Macaque-tropic HIV-1 derivatives: a novel experimental approach to understand viral replication and evolution *in vivo*, p 325–348. *In* Chang T.Y.-L. (ed), HIV-host interactions. InTech, Rijeka, Croatia. http://www.intechopen.com/books/hiv-host-interactions/macaque-tropic-hiv-1-derivatives-a-novel-experimental-approach-to-understand-viral-replication-and-e.
9. **Shedlock DJ, Silvestri G, Weiner DB.** 2009. Monkeying around with HIV vaccines: using rhesus macaques to define 'gatekeepers' for clinical trials. Nat. Rev. Immunol. **9**:717–728.
10. **Nomaguchi M, Doi N, Matsumoto Y, Sakai Y, Fujiwara S, Adachi A.** 2012. Species tropism of HIV-1 modulated by viral accessory proteins. Front. Microbiol. **3**:267. doi:10.3389/fmicb.2012.00267.
11. **Holmes RK, Malim MH, Bishop KN.** 2007. APOBEC-mediated viral restriction: not simply editing? Trends Biochem. Sci. **32**:118–128.
12. **Malim MH, Emerman M.** 2008. HIV-1 accessory proteins—ensuring viral survival in a hostile environment. Cell Host Microbe **3**:388–398.
13. **Grütter MG, Luban J.** 2012. TRIM5 structure, HIV-1 capsid recognition, and innate immune signaling. Curr. Opin. Virol. **2**:142–150.
14. **Nakayama EE, Shioda T.** 2010. Anti-retroviral activity of TRIM5 alpha. Rev. Med. Virol. **20**:77–92.
15. **Douglas JL, Gustin JK, Viswanathan K, Mansouri M, Moses AV, Früh K.** 2010. The great escape: viral strategies to counter BST-2/tetherin. PLoS Pathog. **6**:e1000913. doi:10.1371/journal.ppat.1000913.
16. **Hatziioannou T, Ambrose Z, Chung NP, Piatak M, Jr, Yuan F, Trubey CM, Coalter V, Kiser R, Schneider D, Smedley J, Pung R, Gathuka M, Estes JD, Veazey RS, KewalRamani VN, Lifson JD, Bieniasz PD.** 2009. A macaque model of HIV-1 infection. Proc. Natl. Acad. Sci. U. S. A. **106**:4425–4429.
17. **Hatziioannou T, Princiotta M, Piatak M, Jr, Yuan F, Zhang F, Lifson JD, Bieniasz PD.** 2006. Generation of simian-tropic HIV-1 by restriction factor evasion. Science **314**:95. doi:10.1126/science.1130994.
18. **Kamada K, Igarashi T, Martin MA, Khamsri B, Hatcho K, Yamashita T, Fujita M, Uchiyama T, Adachi A.** 2006. Generation of HIV-1 derivatives that productively infect macaque monkey lymphoid cells. Proc. Natl. Acad. Sci. U. S. A. **103**:16959–16964.
19. **Nomaguchi M, Yokoyama M, Kono K, Nakayama EE, Shioda T, Saito A, Akari H, Yasutomi Y, Matano T, Sato H, Adachi A.** 2013. Gag-CA Q110D mutation elicits TRIM5-independent enhancement of HIV-1mt replication in macaque cells. Microbes Infect. **15**:56–65.
20. **Saito A, Nomaguchi M, Iijima S, Kuroishi A, Yoshida T, Lee YJ, Hayakawa T, Kono K, Nakayama EE, Shioda T, Yasutomi Y, Adachi A, Matano T, Akari H.** 2011. Improved capacity of a monkey-tropic HIV-1 derivative to replicate in cynomolgus monkeys with minimal modifications. Microbes Infect. **13**:58–64.
21. **Thippeshappa R, Polacino P, Yu Kimata MT, Siwak EB, Anderson D, Wang W, Sherwood L, Arora R, Wen M, Zhou P, Hu SL, Kimata JT.** 2011. Vif substitution enables persistent infection of pig-tailed macaques by human immunodeficiency virus type 1. J. Virol. **85**:3767–3779.
22. **Shingai M, Yoshida T, Martin MA, Strebel K.** 2011. Some human immunodeficiency virus type 1 Vpu proteins are able to antagonize macaque BST-2 *in vitro* and *in vivo*: Vpu-negative simian-human immunodeficiency viruses are attenuated *in vivo*. J. Virol. **85**:9708–9715.
23. **Bitzegeio J, Sampias M, Bieniasz PD, Hatziioannou T.** 2013. Adaptation to the interferon-induced antiviral state by human and simian immunodeficiency viruses. J. Virol. **87**:3549–3560.
24. **Saito A, Nomaguchi M, Kono K, Iwatani Y, Yokoyama M, Yasutomi Y, Sato H, Shioda T, Sugiura W, Matano T, Adachi A, Nakayama E, Akari H.** 2013. *TRIM5* genotypes in cynomolgus monkeys primarily influence inter-individual diversity in susceptibility to monkey-tropic human immunodeficiency virus type 1. J. Gen. Virol. **94**:1318–1324.
25. **Doi N, Fujiwara S, Adachi A, Nomaguchi M.** 2011. Rhesus M1.3S cells suitable for biological evaluation of macaque-tropic HIV/SIV clones. Front. Microbiol. **2**:115. doi:10.3389/fmicb.2011.00115.
26. **Sauter D, Schindler M, Specht A, Landford WN, Münch J, Kim KA, Votteler J, Schubert U, Bibollet-Ruche F, Keele BF, Takehisa J, Ogando Y, Ochsenbauer C, Kappes JC, Ayouba A, Peeters M, Learn GH, Shaw G, Sharp PM, Bieniasz P, Hahn BH, Hatziioannou T, Kirchhoff F.** 2009. Tetherin-driven adaptation of Vpu and Nef function and the evolution of pandemic and nonpandemic HIV-1 strains. Cell Host Microbe **6**:409–421.
27. **Lebkowski JS, Clancy S, Calos MP.** 1985. Simian virus 40 replication in adenovirus-transformed human cells antagonizes gene expression. Nature **317**:169–171.
28. **Kimpton J, Emerman M.** 1992. Detection of replication-competent and pseudotyped human immunodeficiency virus with a sensitive cell line on the basis of activation of an integrated beta-galactosidase gene. J. Virol. **66**:2232–2239.
29. **Nomaguchi M, Doi N, Fujiwara S, Fujita M, Adachi A.** 2010. Site-

directed mutagenesis of HIV-1 *vpu* gene demonstrates two clusters of replication-defective mutants with distinct ability to down-modulate cell surface CD4 and tetherin. Front. Microbiol. 1:116. doi:10.3389/fmicb.2010.00116.
30. McNatt MW, Zang T, Hatziioannou T, Bartlett M, Fofana IB, Johnson WE, Neil SJ, Bieniasz PD. 2009. Species-specific activity of HIV-1 Vpu and positive selection of tetherin transmembrane domain variants. PLoS Pathog. 5:e1000300. doi:10.1371/journal.ppat.1000300.
31. Yoshida T, Kao S, Strebel K. 2011. Identification of residues in the BST-2 TM domain important for antagonism by HIV-1 Vpu using a gain-of-function approach. Front. Microbiol. 2:35. doi:10.3389/fmicb.2011.00035.
32. Adachi A, Gendelman HE, Koenig S, Folks T, Willey R, Rabson A, Martin MA. 1986. Production of acquired immunodeficiency syndrome-associated retrovirus in human and nonhuman cells transfected with an infectious molecular clone. J. Virol. 59:284–291.
33. Willey RL, Smith DH, Lasky LA, Theodore TS, Earl PL, Moss B, Capon DJ, Martin MA. 1988. In vitro mutagenesis identifies a region within the envelope gene of the human immunodeficiency virus that is critical for infectivity. J. Virol. 62:139–147.
34. O'Doherty U, Swiggard WJ, Malim MH. 2000. Human immunodeficiency virus type 1 spinoculation enhances infection through virus binding. J. Virol. 74:10074–10080.
35. Wilson SJ, Webb BL, Ylinen LM, Verschoor E, Heeney JL, Towers GJ. 2008. Independent evolution of an antiviral TRIMCyp in rhesus macaques. Proc. Natl. Acad. Sci. U. S. A. 105:3557–3562.
36. Kono K, Song H, Yokoyama M, Sato H, Shioda T, Nakayama EE. 2010. Multiple sites in the N-terminal half of simian immunodeficiency virus capsid protein contribute to evasion from rhesus monkey TRIM5α-mediated restriction. Retrovirology 7:72. doi:10.1186/1742-4690-7-72.
37. Howard BR, Vajdos FF, Li S, Sundquist WI, Hill CP. 2003. Structural insights into the catalytic mechanism of cyclophilin A. Nat. Struct. Biol. 10:475–481.
38. Park SH, Mrse AA, Nevzorov AA, Mesleh MF, Oblatt-Montal M, Montal M, Opella SJ. 2003. Three-dimensional structure of the channel-forming trans-membrane domain of virus protein "u" (Vpu) from HIV-1. J. Mol. Biol. 333:409–424.
39. Leaver-Fay A, Tyka M, Lewis SM, Lange OF, Thompson J, Jacak R, Kaufman K, Renfrew PD, Smith CA, Sheffler W, Davis IW, Cooper S, Treuille A, Mandell DJ, Richter F, Ban YE, Fleishman SJ, Corn JE, Kim DE, Lyskov S, Berrondo M, Mentzer S, Popović Z, Havranek JJ, Karanicolas J, Das R, Meiler J, Kortemme T, Gray JJ, Kuhlman B, Baker D, Bradley P. 2011. ROSETTA3: an object-oriented software suite for the simulation and design of macromolecules. Methods Enzymol. 487:545–574.
40. Kirmaier A, Wu F, Newman RM, Hall LR, Morgan JS, O'Connor S, Marx PA, Meythaler M, Goldstein S, Buckler-White A, Kaur A, Hirsch VM, Johnson WE. 2010. *TRIM5* suppresses cross-species transmission of a primate immunodeficiency virus and selects for emergence of resistant variants in the new species. PLoS Biol. 8:e1000462. doi:10.1371/journal.pbio.1000462.
41. Newman RM, Hall L, Connole M, Chen GL, Sato S, Yuste E, Diehl W, Hunter E, Kaur A, Miller GM, Johnson WE. 2006. Balancing selection and the evolution of functional polymorphism in Old World monkey TRIM5alpha. Proc. Natl. Acad. Sci. U. S. A. 103:19134–19139.
42. Price AJ, Marzetta F, Lammers M, Ylinen LM, Schaller T, Wilson SJ, Towers GJ, James LC. 2009. Active site remodeling switches HIV specificity of antiretroviral TRIMCyp. Nat. Struct. Mol. Biol. 16:1036–1042.
43. Ylinen LM, Price AJ, Rasaiyaah J, Hué S, Rose NJ, Marzetta F, James LC, Towers GJ. 2010. Conformational adaptation of Asian macaque TRIMCyp directs lineage specific antiviral activity. PLoS Pathog. 6:e1001062. doi:10.1371/journal.ppat.1001062.
44. Fassati A. 2012. Multiple roles of the capsid protein in the early steps of HIV-1 infection. Virus Res. 170:15–24.
45. Ganser-Pornillos BK, Yeager M, Sundquist WI. 2008. The structural biology of HIV assembly. Curr. Opin. Struct. Biol. 18:203–217.
46. Miyamoto T, Yokoyama M, Kono K, Shioda T, Sato H, Nakayama EE. 2011. A single amino acid of human immunodeficiency virus type 2 capsid protein affects conformation of two external loops and viral sensitivity to TRIM5α. PLoS One 6:e22779. doi:10.1371/journal.pone.0022779.
47. Nomaguchi M, Doi N, Fujiwara S, Saito A, Akari H, Nakayama EE, Shioda T, Yokoyama M, Sato H, Adachi A. 2013. Systemic biological analysis of the mutations in two distinct HIV-1mt genomes occurred during replication in macaque cells. Microbes Infect. 15:319–328.
48. Hatziioannou T, Cowan S, Von Schwedler UK, Sundquist WI, Bieniasz PD. 2004. Species-specific tropism determinants in the human immunodeficiency virus type 1 capsid. J. Virol. 78:6005–6012.
49. Owens CM, Song B, Perron MJ, Yang PC, Stremlau M, Sodroski J. 2004. Binding and susceptibility to postentry restriction factors in monkey cells are specified by distinct regions of the human immunodeficiency virus type 1 capsid. J. Virol. 78:5423–5437.
50. von Schwedler UK, Stray KM, Garrus JE, Sundquist WI. 2003. Functional surfaces of the human immunodeficiency virus type 1 capsid protein. J. Virol. 77:5439–5450.
51. Lim SY, Rogers T, Chan T, Whitney JB, Kim J, Sodroski J, Letvin NL. 2010. TRIM5alpha modulates immunodeficiency virus control in rhesus monkeys. PLoS Pathog. 6:e1000738. doi:10.1371/journal.ppat.1000738.
52. Jia B, Serra-Moreno R, Neidermyer W, Rahmberg A, Mackey J, Fofana IB, Johnson WE, Westmoreland S, Evans DT. 2009. Species-specific activity of SIV Nef and HIV-1 Vpu in overcoming restriction by tetherin/BST2. PLoS Pathog. 5:e1000429. doi:10.1371/journal.ppat.1000429.
53. Zhang F, Wilson SJ, Landford WC, Virgen B, Gregory D, Johnson MC, Munch J, Kirchhoff F, Bieniasz PD, Hatziioannou T. 2009. Nef proteins from simian immunodeficiency viruses are tetherin antagonists. Cell Host Microbe 6:54–67.
54. Vigan R, Neil SJ. 2010. Determinants of tetherin antagonism in the transmembrane domain of the human immunodeficiency virus type 1 Vpu protein. J. Virol. 84:12958–12970.
55. McCarthy KR, Schmidt AG, Kirmaier A, Wyand AL, Newman RM, Johnson WE. 2013. Gain-of-sensitivity mutations in a Trim5-resistant primary isolate of pathogenic SIV identify two independent conserved determinants of Trim5α specificity. PLoS Pathog. 9:e1003352. doi:10.1371/journal.ppat.1003352.
56. Kuroishi A, Saito A, Shingai Y, Shioda T, Nomaguchi M, Adachi A, Akari H, Nakayama EE. 2009. Modification of a loop sequence between alpha-helices 6 and 7 of virus capsid (CA) protein in a human immunodeficiency virus type 1 (HIV-1) derivative that has simian immunodeficiency virus (SIVmac239) vif and CA alpha-helices 4 and 5 loop improves replication in cynomolgus monkey cells. Retrovirology 6:70. doi:10.1186/1742-4690-6-70.
57. Ohkura S, Goldstone DC, Yap MW, Holden-Dye K, Taylor IA, Stoye JP. 2011. Novel escape mutants suggest an extensive TRIM5α binding site spanning the entire outer surface of the murine leukemia virus capsid protein. PLoS Pathog. 7:e1002011. doi:10.1371/journal.ppat.1002011.
58. Homann S, Smith D, Little S, Richman D, Guatelli J. 2011. Upregulation of BST-2/tetherin by HIV infection *in vivo*. J. Virol. 85:10659–10668.
59. Liberatore RA, Bieniasz PD. 2011. Tetherin is a key effector of the antiretroviral activity of type I interferon in vitro and in vivo. Proc. Natl. Acad. Sci. U. S. A. 108:18097–18101.
60. Pillai SK, Abdel-Mohsen M, Guatelli J, Skasko M, Monto A, Fujimoto K, Yukl S, Greene WC, Kovari H, Rauch A, Fellay J, Battegay M, Hirschel B, Witteck A, Bernasconi E, Ledergerber B, Günthard HF, Wong JK, Swiss HIV Cohort Study. 2012. Role of retroviral restriction factors in the interferon-α-mediated suppression of HIV-1 in vivo. Proc. Natl. Acad. Sci. U. S. A. 109:3035–3040.
61. Serra-Moreno R, Jia B, Breed M, Alvarez X, Evans DT. 2011. Compensatory changes in the cytoplasmic tail of gp41 confer resistance to tetherin/BST-2 in a pathogenic nef-deleted SIV. Cell Host Microbe 9:46–57.
62. Goldstein S, Brown CR, Dehghani H, Lifson JD, Hirsch VM. 2000. Intrinsic susceptibility of rhesus macaque peripheral CD4(+) T cells to simian immunodeficiency virus in vitro is predictive of in vivo viral replication. J. Virol. 74:9388–9395.
63. Lifson JD, Nowak MA, Goldstein S, Rossio JL, Kinter A, Vasquez G, Wiltrout TA, Brown C, Schneider D, Wahl L, Lloyd AL, Williams J, Elkins WR, Fauci AS, Hirsch VM. 1997. The extent of early viral replication is a critical determinant of the natural history of simian immunodeficiency virus infection. J. Virol. 71:9508–9514.
64. Igarashi T, Iyengar R, Byrum RA, Buckler-White A, Dewar RL, Buckler CE, Lane HC, Kamada K, Adachi A, Martin MA. 2007. Human immunodeficiency virus type 1 derivative with 7% simian immunodeficiency virus genetic content is able to establish infections in pig-tailed macaques. J. Virol. 81:11549–11552.
65. Lifson JD, Haigwood NL. 2012. Lessons in nonhuman primate models for AIDS vaccine research: from minefields to milestones. Cold Spring Harb. Perspect. Med. 2:a007310. doi:10.1101/cshperspect.a007310.
66. Shaw GM, Hunter E. 2012. HIV transmission. Cold Spring Harb. Perspect. Med. 2:a006965. doi:10.1101/cshperspect.a006965.

67. Swanstrom R, Coffin J. 2012. HIV-1 pathogenesis: the virus. Cold Spring Harb. Perspect. Med. 2:a007443. doi:10.1101/cshperspect.a007443.
68. Nishimura Y, Shingai M, Willey R, Sadjadpour R, Lee WR, Brown CR, Brenchley JM, Buckler-White A, Petros R, Eckhaus M, Hoffman V, Igarashi T, Martin MA. 2010. Generation of the pathogenic R5-tropic simian/human immunodeficiency virus $SHIV_{AD8}$ by serial passaging in rhesus macaques. J. Virol. 84:4769–4781.
69. Ren W, Mumbauer A, Gettie A, Seaman MS, Russell-Lodrigue K, Blanchard J, Westmoreland S, Cheng-Mayer C. 2013. Generation of lineage-related, mucosally transmissible subtype C R5 simian-human immunodeficiency viruses capable of AIDS development, induction of neurological disease, and coreceptor switching in rhesus macaques. J. Virol. 87:6137–6149.
70. Shingai M, Donau OK, Schmidt SD, Gautam R, Plishka RJ, Buckler-White A, Sadjadpour R, Lee WR, LaBranche CC, Montefiori DC, Mascola JR, Nishimura Y, Martin MA. 2012. Most rhesus macaques infected with the CCR5-tropic $SHIV_{AD8}$ generate cross-reactive antibodies that neutralize multiple HIV-1 strains. Proc. Natl. Acad. Sci. U. S. A. 109:19769–19774.
71. Shibata R, Kawamura M, Sakai H, Hayami M, Ishimoto A, Adachi A. 1991. Generation of a chimeric human and simian immunodeficiency virus infectious to monkey peripheral blood mononuclear cells. J. Virol. 65:3514–3520.
72. Kawamura M, Sakai H, Adachi A. 1994. Human immunodeficiency virus Vpx is required for the early phase of replication in peripheral blood mononuclear cells. Microbiol. Immunol. 38:871–878.
73. Gamble TR, Vajdos FF, Yoo S, Worthylake DK, Houseweart M, Sundquist WI, Hill CP. 1996. Crystal structure of human cyclophilin A bound to the amino-terminal domain of HIV-1 capsid. Cell 87:1285–1294.

Anti-CCR4 mAb selectively depletes effector-type FoxP3$^+$CD4$^+$ regulatory T cells, evoking antitumor immune responses in humans

Daisuke Sugiyama[a], Hiroyoshi Nishikawa[a,1], Yuka Maeda[a], Megumi Nishioka[a,b], Atsushi Tanemura[b], Ichiro Katayama[b], Sachiko Ezoe[c], Yuzuru Kanakura[c], Eiichi Sato[d], Yasuo Fukumori[e], Julia Karbach[f], Elke Jäger[f], and Shimon Sakaguchi[a,1]

[a]Experimental Immunology, World Premier International Research Center, Immunology Frontier Research Center, [b]Department of Dermatology, and [c]Department of Hematology and Oncology, Graduate School of Medicine, Osaka University, Osaka 565-0871, Japan; [d]Department of Anatomic Pathology, Tokyo Medical University, Tokyo 160-8402, Japan; [e]The Third Section of Clinical Investigation, Kinki Blood Center, Osaka 536-8505, Japan; and [f]Department of Hematology and Oncology, Krankenhaus Nordwest, Frankfurt 60488, Germany

Contributed by Shimon Sakaguchi, September 23, 2013 (sent for review June 27, 2013)

CD4$^+$ Treg cells expressing the transcription factor FOXP3 (forkhead box P3) are abundant in tumor tissues and appear to hinder the induction of effective antitumor immunity. A substantial number of T cells, including Treg cells, in tumor tissues and peripheral blood express C-C chemokine receptor 4 (CCR4). Here we show that CCR4 was specifically expressed by a subset of terminally differentiated and most suppressive CD45RA$^-$FOXP3^{hi}CD4$^+$ Treg cells [designated effector Treg (eTreg) cells], but not by CD45RA$^+$FOXP3^{lo}CD4$^+$ naive Treg cells, in peripheral blood of healthy individuals and cancer patients. In melanoma tissues, CCR4$^+$ eTreg cells were predominant among tumor-infiltrating FOXP3$^+$ T cells and much higher in frequency compared with those in peripheral blood. With peripheral blood lymphocytes from healthy individuals and melanoma patients, ex vivo depletion of CCR4$^+$ T cells and subsequent in vitro stimulation of the depleted cell population with the cancer/testis antigen NY-ESO-1 efficiently induced NY-ESO-1–specific CD4$^+$ T cells. Nondepletion failed in the induction. The magnitude of the responses was comparable with total removal of FOXP3$^+$ Treg cells by CD25$^+$ T-cell depletion. CCR4$^+$ T-cell depletion also augmented in vitro induction of NY-ESO-1–specific CD8$^+$ T cells in melanoma patients. Furthermore, in vivo administration of anti-CCR4 mAb markedly reduced the eTreg-cell fraction and augmented NY-ESO-1–specific CD8$^+$ T-cell responses in an adult T-cell leukemia-lymphoma patient whose leukemic cells expressed NY-ESO-1. Collectively, these findings indicate that anti-CCR4 mAb treatment is instrumental for evoking and augmenting antitumor immunity in cancer patients by selectively depleting eTreg cells.

cancer immunotherapy | immunomodulation

Naturally occurring CD25$^+$CD4$^+$ regulatory T (Treg) cells expressing the transcription factor forkhead box P3 (FOXP3) are indispensable for the maintenance of immunological self-tolerance and homeostasis (1, 2). Given that most tumor-associated antigens are antigenically normal self-constituents (3–5), it is likely that natural FOXP3$^+$ Treg cells engaged in self-tolerance concurrently hinder immune surveillance against cancer in healthy individuals and also hamper the development of effective antitumor immunity in tumor-bearing patients. Indeed FOXP3$^+$CD25$^+$CD4$^+$ Treg cells are abundant in tumor tissues (6–10), and their depletion augments spontaneous and vaccine-induced antitumor immune responses in animal models (10, 11). In humans, increased numbers of FOXP3$^+$CD25$^+$CD4$^+$ Treg cells and, in particular, decreased ratios of CD8$^+$ T cells to FOXP3$^+$CD25$^+$CD4$^+$ Treg cells among tumor-infiltrating lymphocytes (TIL) are well correlated with poor prognosis in various types of cancers (6, 7, 10). Some clinical studies have shown the potential of depleting CD25-expressing lymphocytes to augment antitumor immune responses (12, 13); yet other similar studies failed to support the effects (10, 14, 15). Because activated effector T cells also express CD25, and their production of IL-2 is required for the expansion of CD8$^+$ cytotoxic lymphocytes, CD25-based cell depletion may reduce activated effector T cells as well, cancelling the effect of Treg-cell depletion to augment antitumor immunity (10). In addition, it has been demonstrated in animal models that depletion of Treg cells as a whole can trigger autoimmunity (1, 16, 17). Therefore, a current key issue is to determine how Treg cells can be controlled to evoke and enhance antitumor immunity without affecting effector T cells or eliciting deleterious autoimmunity.

Human FOXP3$^+$CD4$^+$ T cells are heterogenous in phenotype and function (2). These cells can be dissected into three subpopulations by the expression levels of FOXP3 and the cell-surface molecules CD45RA and CD25: (*i*) FOXP3^{hi}CD45RA$^-$CD25^{hi} cells, designated effector Treg (eTreg) cells, which are terminally differentiating and highly suppressive; (*ii*) FOXP3^{lo}CD45RA$^+$CD25^{lo} cells, designated naive Treg cells, which differentiate into eTreg cells upon antigenic stimulation; and (*iii*) FOXP3^{lo}CD45RA$^-$CD25^{lo} non-Treg cells, which do not possess suppressive activity but secrete proinflammatory cytokines (18). In principle, these distinct properties of FOXP3$^+$ T-cell subpopulations can be exploited to augment antitumor immunity without inducing autoimmunity, for example, by depleting a particular Treg-cell subpopulation rather than whole Foxp3$^+$-cell population. One of

Significance

Regulatory T (Treg) cells expressing the transcription factor FOXP3 play a critical role in suppressing antitumor immune responses. Here we found that, compared with peripheral blood T cells, tumor-infiltrating T cells contained a higher frequency of effector Tregs, which are defined as FOXP3^{hi} and CD45RA$^-$, terminally differentiated, and most suppressive. Effector Treg cells, but not FOXP3^{lo} and CD45RA$^+$ naïve Treg cells, predominantly expressed C-C chemokine receptor 4 (CCR4) in both cancer tissues and peripheral blood. In vivo or in vitro anti-CCR4 mAb treatment selectively depleted effector Treg cells and efficiently induced tumor-antigen-specific CD4$^+$ and CD8$^+$ T cells. Thus, cell-depleting anti-CCR4 mAb therapy is instrumental for evoking and enhancing tumor immunity in humans via selectively removing effector-type FOXP3$^+$ Treg cells.

Author contributions: H.N. and S.S. designed research; D.S., H.N., Y.M., E.S., and Y.F. performed research; M.N., A.T., I.K., S.E., Y.K., J.K., and E.J. contributed new reagents/analytic tools; D.S., H.N., Y.M., and S.S. analyzed data; D.S., H.N., Y.M., and S.S. wrote the paper; and M.N., A.T., I.K., S.E., Y.K., J.K., and E.J. collected clinical samples and data.

Conflict of interest statement: H.N. received a research grant from Kyowa Hakko Kirin Co., Ltd.

[1]To whom correspondence may be addressed. E-mail: nisihiro@ifrec.osaka-u.ac.jp or shimon@ifrec.osaka-u.ac.jp.

This article contains supporting information online at www.pnas.org/lookup/suppl/doi:10.1073/pnas.1316796110/-/DCSupplemental.